

ปริมาณรังสีและคุณภาพของภาพในการตรวจหลอดเลือดโคโรนารี จากเครื่องคอมพิวเตอร์โทโม  
กราฟฟี ชนิด 320 แถวของหัววัด

นางสาวจุฑารัตน์ ถนอมพุดซา

วิทยานิพนธ์นี้เป็นส่วนหนึ่งของการศึกษาตามหลักสูตรปริญญาวิทยาศาสตรมหาบัณฑิต  
สาขาวิชาฉายาเวชศาสตร์ ภาควิชารังสีวิทยา  
คณะแพทยศาสตร์ จุฬาลงกรณ์มหาวิทยาลัย  
ปีการศึกษา 2554  
ลิขสิทธิ์ของจุฬาลงกรณ์มหาวิทยาลัย

บทคัดย่อและแฟ้มข้อมูลฉบับเต็มของวิทยานิพนธ์ตั้งแต่ปีการศึกษา 2554 ที่ให้บริการในคลังปัญญาจุฬาฯ (CUIR)  
เป็นแฟ้มข้อมูลของนิสิตเจ้าของวิทยานิพนธ์ที่ส่งผ่านทางบัณฑิตวิทยาลัย

The abstract and full text of theses from the academic year 2011 in Chulalongkorn University Intellectual Repository (CUIR)  
are the thesis authors' files submitted through the Graduate School.

**RADIATION DOSE AND IMAGE QUALITY FROM CORONARY  
ANGIOGRAPHY IN 320-DETECTOR ROW COMPUTED  
TOMOGRAPHY**

**Miss Jutharat Thanomphudsa**

**A Thesis Submitted in Partial Fulfillment of the Requirements  
for the Degree of Master of Science Program in Medical Imaging**

**Department of Radiology**

**Faculty of Medicine**

**Chulalongkorn University**

**Academic Year 2011**

**Copyright of Chulalongkorn University**

Thesis Title                      RADIATION DOSE AND IMAGE QUALITY FROM  
CORONARY ANGIOGRAPHY IN 320-DETECTOR ROW  
COMPUTED TOMOGRAPHY

By                                      Miss Jutharat Thanomphudsa


Field of Study                      Medical Imaging

Thesis Advisor                      Associate Professor Anchali Krisanachinda, Ph.D.


Thesis Co-advisor                      Monravee Tumkosit, M.D.

---


Accepted by the Faculty of Medicine, Chulalongkorn University in  
Partial Fulfillment of the Requirements for the Master's Degree


.....Dean of the Faculty of Medicine  
(Associate Professor Sophon Napathorn, M.D.)

THESIS COMMITTEE

.....Chairman  
(Associate Professor Somjai Wangsuphachart, M.D.)

.....Thesis Advisor  
(Associate Professor Anchali Krisanachinda, Ph.D.)


.....Thesis Co-advisor  
(Monravee Tumkosit, M.D.)


..... External Examiner  
(Professor Franco Milano, Ph.D.)

จุฬารัตน์ ดนอมพุดชา : ปริมาณรังสีและคุณภาพของภาพในการตรวจหลอดเลือดโคโรนารี จากเครื่องคอมพิวเตอร์ ตัดโทโมกราฟี ชนิด 320 แถวของหัววัด. (RADIATION DOSE AND IMAGE QUALITY FROM CORONARY ANGIOGRAPHY IN 320-DETECTOR ROW COMPUTED TOMOGRAPHY) อ.ที่ปรึกษาวิทยานิพนธ์หลัก : รศ.ดร.อัญชลี กฤษณจินดา. 74 หน้า.

ในปัจจุบันการตรวจหลอดเลือดหัวใจโคโรนารี จากเครื่องเอกซเรย์คอมพิวเตอร์หรือเครื่องคอมพิวเตอร์ตัดโทโมกราฟี หรือ ซีทีที่มีอัตราเพิ่มขึ้นอย่างรวดเร็ว เครื่องซีทีมีการพัฒนาเพื่อให้ได้ภาพที่มีคุณภาพดีขึ้นในขณะที่ผู้ป่วยได้รับปริมาณรังสีน้อยลง การศึกษาวิจัยนี้เพื่อจะประเมินปริมาณรังสีและคุณภาพของภาพที่ผู้ป่วยได้รับจากการตรวจหลอดเลือดโคโรนารีจากเครื่อง ซีทีชนิด 320 แถวของหัววัด โดยศึกษาในผู้ป่วยจำนวน 41 รายที่มารับการตรวจที่โรงพยาบาลจุฬาลงกรณ์ สภากาชาดไทย ในการตรวจนี้ ใช้เครื่องซีทีชนิด 320 แถวของหัววัดผลิตภัณฑ์โคชิบา รุ่น Aquilion ONE ประเมินปริมาณรังสีและคุณภาพของภาพ ผู้ป่วย จะได้รับการตรวจโดยโปรโตคอลที่ใช้ขึ้นอยู่กับอัตราการเต้นของหัวใจ ถ้าอัตราการเต้นของหัวใจน้อยกว่าหรือเท่ากับ 65 ครั้งต่อนาทีใช้การตรวจแบบโปรสเปคทีฟเฟท 70-80% 1 รอบ ถ้าอัตราการเต้นของหัวใจอยู่ระหว่าง 66-70 ครั้งต่อนาทีใช้การตรวจแบบโปรสเปคทีฟเฟท 30-80% 1 รอบ อัตราการเต้นของหัวใจ 71-75 ครั้งต่อนาทีใช้การตรวจแบบโปรสเปคทีฟเฟท 30-80% 2 รอบ และถ้าอัตราการเต้นของหัวใจมากกว่า 75 ครั้งต่อนาทีใช้การตรวจแบบรีโทรสเปคทีฟเฟทแบบปรับกระแสหลอด และทำการบันทึกค่าเควีพี, มิลลิแอมแปร์, อัตราการเต้นของหัวใจ, คำนิมวลกาย, CTDI<sub>vol</sub> และ DLP การตั้งค่า มิลลิแอมแปร์ และ เควีพีขึ้นอยู่กับค่านิมวลกายของผู้ป่วย ปริมาณรังสียังผลได้จากการคำนวณจากค่า DLP และค่าคอนเวอร์ชันแฟคเตอร์ ส่วนคุณภาพของภาพประเมินโดยรังสีแพทย์ 2 ท่าน และศึกษาภาพเชิงปริมาณโดยใช้ค่า noise ร่วมด้วย

จากผลการศึกษาพบว่าปริมาณรังสีเฉลี่ยที่ผู้ป่วยได้รับจากการใช้โปรสเปคทีฟเฟท 70-80% คือ  $3.6 \pm 0.9$  มิลลิซีเวิร์ท จากการตรวจแบบโปรสเปคทีฟเฟท 30-80% 1 รอบ คือ  $6.3 \pm 1.9$  มิลลิซีเวิร์ท จากการตรวจแบบโปรสเปคทีฟเฟท 30-80% 2 รอบ คือ  $10.8 \pm 1.8$  มิลลิซีเวิร์ท และจากการตรวจแบบรีโทรสเปคทีฟเฟทแบบปรับกระแสหลอด คือ  $12.1 \pm 7.7$  มิลลิซีเวิร์ท ค่า noise สูงที่สุดในการตรวจแบบโปรสเปคทีฟเฟท 70-80% และลดลงในการตรวจแบบรีโทรสเปคทีฟเฟทแบบปรับกระแสหลอด โปรสเปคทีฟเฟท 30-80% 1 รอบ และแบบโปรสเปคทีฟเฟท 30-80% 2 รอบ ตามลำดับ ส่วนคุณภาพของภาพที่ได้อยู่ในเกณฑ์ดีถึงดีมาก การเต้นของหัวใจ การแปรผันในการเต้นของหัวใจและโรคของผู้ป่วยนั้นมีผลต่อปริมาณรังสีและคุณภาพของภาพที่ได้รับ ดังนั้นการเลือกโปรโตคอลที่เหมาะสมจึงเป็นสิ่ง จำเป็นอย่างยิ่ง สรุปได้ว่าการตรวจหลอดเลือดหัวใจโคโรนารีจากเครื่องซีทีชนิด 320 แถวของหัววัดนี้ได้ภาพที่ดีถึงดีมากและยังได้รับปริมาณรังสีที่น้อยกว่าที่เคยมีในรายงาน โดยเฉพาะอย่างยิ่งในการตรวจแบบโปรสเปคทีฟเฟทเมื่อเปรียบเทียบกับแบบรีโทรสเปคทีฟเฟท การควบคุมให้อัตราการเต้นของหัวใจผู้ป่วยให้ช้า(65 ครั้งต่อนาที)อยู่ในเกณฑ์ที่ใช้โปรสเปคทีฟเฟท 70-80% จึงยังมีความสำคัญเพื่อให้ผู้ป่วยได้รับรังสีน้อยที่สุด และควรเลือกใช้โปรโตคอลที่มีช่วงการปล่อยรังสีแคบกว่าและตรวจ 1 รอบการเต้นของหัวใจควรใช้เพื่อเป็นประโยชน์กับผู้ป่วย

ภาควิชา .....รังสีวิทยา..... ลายมือชื่อนิสิต..... 

สาขาวิชา .....ฉายาเวชศาสตร์..... ลายมือชื่อ อ. ที่ปรึกษาวิทยานิพนธ์หลัก..... 

ปีการศึกษา .....2554.....



##5374620030 : MAJOR MEDICAL IMAGING  
KEYWORDS : EFFECTIVE DOSE/ DOSE LENGTH PRODUCT/ COMPUTED TOMOGRAPHY DOSE INDEX/ CORONARY COMPUTED TOMOGRAPHY ANGIOGRAPHY

JUTHARAT THANOMPHUDSA: RADIATION DOSE AND IMAGE QUALITY FROM CORONARY ANGIOGRAPHY IN 320-DETECTOR ROW COMPUTED TOMOGRAPHY. ADVISOR: ASSOC.PROF. ANCHALI KRISANACHINDA, Ph.D., 74 pp.

Coronary Computed Tomography Angiography (CCTA) examinations are increasing rapidly. Computed Tomography (CT) has been developed to improve image quality with the patient dose reduction. The purpose of this study is to evaluate radiation dose and image quality of CCTA in patients using 320-detector row CT. Forty-one patients referred for cardiac CT examinations at King Chulalongkorn Memorial Hospital were included in this study. All CCTA examinations were performed on the 320-detector row CT, Toshiba Aquilion ONE. Scanning protocol was investigated on dose estimates and image quality. Patients were scanned based on heart rate (HR) by  $HR \leq 65$  bpm, using prospective gating 70-80% of R-R interval of cardiac cycle (1 heart beat),  $HR 66 - 70$  bpm, using prospective gating 30 -80 % R-R(1 heart beat),  $HR 71 - 74$  bpm, using prospective gating 30 -80 % R-R(2 heart beats) and  $HR \geq 75$  bpm using retrospective with dose modulation. Scanning parameters, kVp, mA, HR, BMI,  $CTDI_{vol}(mGy)$  and  $DLP(mGy.cm)$  were recorded to study the factors affecting the image quality and patient dose. The mA and kVp settings depend on BMI of the patient. Effective dose was calculated from DLP using specific conversion factor. The image quality was evaluated by two radiologists. Noise assessment was also studied quantitatively.

The results show patient effective dose in prospective gating technique (PGT) 70-80% R-R interval as  $3.6 \pm 0.9$  mSv, prospective gating 30-80% (1R-R) =  $6.3 \pm 1.9$  mSv, 30-80% (2R-R) =  $10.8 \pm 1.8$  mSv and in retrospective gating technique (RGT) with tube current modulation =  $12.1 \pm 7.7$  mSv. Image noise was highest in PGT 70-80% (1R-R) and decreasing in orderly from RGT with tube current modulation to PGT 30-80% (1R-R) and the lowest in PGT 30-80% (2R-R). Overall qualitative image quality was mostly good to excellent scores. The heart rate, heart rate variability and disease of the patient affected in the radiation dose and image quality so the suitable acquisition protocols used are necessary. In conclusion, for cardiac CTA in 320-detector row, good to excellent image quality and patient dose reduction during CCTA are obtained especially in prospective technique when compared to earlier designed MDCTs using retrospective technique. The narrowing phase window width and single heart beat could be used for advantage of patient. Pre-examination HR controlling less than 65% R-R interval is still necessary for the highest dose reduction.

Department.....Radiology.....Student's Signature.....*Jutarat Th.*  
Field of Study.....Medical Imaging.....Advisor's Signature.....*Anchal Kr.*  
Academic Year.....2011.....

## ACKNOWLEDGEMENTS

I would like to express thankfulness and deepest appreciation to Associate Professor Anchali Krisanachinda, Ph.D., Division of Nuclear Medicine, Department of Radiology, Faculty of Medicine, Chulalongkorn University, my advisor for her helpful, suggestion, supervision, guidance, constructive direction and polishing of the thesis writing to improve the English expression.

I am greatly grateful to Associate Professor Sivalee Suriyapee, Chief Physicist at Division of Radiation Oncology, Department of Radiology, Faculty of Medicine, Chulalongkorn University, my teacher for her invaluable guidance, constructive direction and encouragement.

I would like to extremely thank Ms. Monravee Tumkosit, M.D., Department of Radiology, Faculty of Medicine, Chulalongkorn University, for an instructor in her advices, helpful, suggestion and guidance to improve protocol and opinion in image quality in this research.

I would like to deeply thank Associate Professor Somjai Wangsuphachart, M.D., Department of Radiology, Faculty of Medicine, Chulalongkorn University, for her helpful suggestion, constructive comments and opinion in image quality in this research.

I would like to thank Mr. Wallop Makmool, Ms. Petcharleeya Suwanpradit, Ms. Walaiporn Kuenkaew, Physicists and technologists at the Unit of Computed Tomography, Mr. Taweap Sanghangthum, Mr. Sornjarod Oonsiri at Division of Radiation Oncology and Mr. Kitiwat Khamwan, Department of Radiology, King Chulalongkorn Memorial Hospital, for their guidance of using machine, facilitating on protocol in this research, useful advices and encouragement.

I am extremely thankful Associate Professor Katsumi Tsujioka, Faculty of Radiological Technology, School of Health Sciences, Fujita Health University, Japan for his teaching of knowledge in Computed Tomography and truthfulness in sharing useful experiences of my research.

I would like to thank Professor Franco Milano, University of Florence Italy, who is the external examiner of the thesis defense for his constructive comments, recommendation and teaching of knowledge in Medical Imaging.

I am thankful for all teachers, lecturers and staff at Master of Science Program in Medical Imaging, Faculty of Medicine, Chulalongkorn University for their suggestions and teaching knowledge during the course of Medical Imaging.

Finally, I am greatly thankful to my family for their invaluable encouragement, entirely care, financial support and understanding during the entire course of the study.

# CONTENTS

	<b>Page</b>
ABSTRACT (THAI).....	iv
ABSTRACT (ENGLISH).....	v
ACKNOWLEDGEMENTS.....	vi
CONTENTS.....	vii
LIST OF TABLES.....	ix
LIST OF FIGURES.....	x
LIST OF ABBREVIATIONS.....	xi
<b>CHAPTER I: INTRODUCTION</b> .....	<b>1</b>
1.1 Background and rationale.....	1
1.2 Objectives.....	2
1.3 Definitions.....	2
<b>CHAPTER II: REVIEW OF RELATED LITERATURES</b> .....	<b>4</b>
2.1 Theory.....	4
2.1.1 The introduction of Computed Tomography (CT).....	4
2.1.2 Image formation.....	5
2.1.3 Multiple Detectors CT (MDCT).....	6
2.1.4 Scan time and scan length.....	7
2.1.5 Image quality.....	8
2.1.6 Ionizing radiation and patient dose.....	11
2.1.7 Automatic tube current control in CT.....	12
2.1.8 Cardiac scanning.....	12
2.1.9 Factors influenced the temporal resolution.....	15
2.1.10 Gantry rotation time.....	15
2.1.11 Acquisition mode.....	15
2.1.12 Reconstruction method.....	17
2.2 Review of related literatures.....	18
<b>CHAPTER III: RESEARCH METHODOLOGY</b> .....	<b>21</b>
3.1 Research design.....	21
3.2 Research design model.....	21
3.3 Conceptual framework.....	21
3.4 Key words.....	22
3.5 Research question.....	22
3.6 Materials.....	22
3.6.1 CT scanner: Toshiba Aquilion ONE.....	22
3.6.2 CT Phantom.....	22
3.6.3 Catphan <sup>®</sup> 600 phantom.....	23
3.6.4 Unfors model Xi platinum dosemeter.....	24
3.6.5 CT pencil-type ionization chamber.....	24
3.6.6 Patients.....	26
3.7 Methods.....	26
3.7.1 Perform the quality control of Toshiba Aquilion ONE.....	26
3.7.2 Verification of CTDIvol and DLP.....	26
3.7.3 Study in Coronary CTA patients.....	26
3.7.4 Data recording.....	27
3.7.5 Evaluate the qualitative image quality.....	27

	<b>Page</b>
3.7.6 Evaluate the quantitative image quality.....	28
3.7.7 Effective dose calculation.....	28
3.8 Sample size.....	28
3.9 Measurement.....	28
3.10 Statistical analysis.....	29
3.11 Data collection.....	29
3.12 Data analysis.....	29
3.13 Outcomes.....	29
3.14 Expected benefits.....	30
3.15 Ethical consideration.....	30
<b>CHAPTER IV: RESULTS.....</b>	<b>31</b>
4.1 Quality control of the CT scanner: TOSHIBA Aquilion ONE.....	31
4.2 Verification of Computed Tomography Dose Index (CTDI).....	32
4.2.1 CTDI <sub>100</sub> in air.....	32
4.2.2 CTDI <sub>100</sub> in head phantom.....	33
4.2.3 CTDI <sub>100</sub> in body phantom.....	33
4.2.4 CTDI <sub>vol</sub> of monitor and calculated CTDI <sub>w</sub> .....	34
4.3 Patient information and scanning parameter.....	36
4.4 Radiation dose.....	38
4.5 Image quality.....	42
4.5.1 Quantitative image quality.....	42
4.5.2 Qualitative image quality.....	43
<b>CHAPTER V: DISCUSSION AND CONCLUSION.....</b>	<b>45</b>
5.1 Discussion.....	45
5.2 Conclusions.....	47
5.3 Recommendation.....	48
<b>REFERENCES.....</b>	<b>49</b>
<b>APPENDICES.....</b>	<b>52</b>
Appendix A: Case record form.....	53
Appendix B: Quality control of computed tomography system.....	55
Appendix C: Patient information sheet and consent form.....	66
<b>VITAE.....</b>	<b>74</b>



## LIST OF TABLES

<b>Table</b>	<b>Page</b>
3.1 Characteristics of Unfors model Xi platinum dosimeter.....	25
3.2 mA and kVp setting.....	27
4.1 Report of CT system performance.....	31
4.2 The measured CTDI <sub>100</sub> in air for head and body protocols for each kVp.....	32
4.3 The measured CTDI <sub>100</sub> at each position of head phantom for each kVp.....	33
4.4 The measured CTDI <sub>100</sub> at each position of body phantom for each kVp.....	33
4.5 CTDI <sub>vol</sub> of monitor and CTDI <sub>w</sub> using head techniques mAs 100, collimation 8 mm and 180 mmFOV.....	34
4.6 CTDI <sub>vol</sub> of monitor and CTDI <sub>w</sub> using body techniques mAs 100, collimation 8 mm and 500 mmFOV.....	35
4.7 Patient information and scanning parameter.....	36
4.8 CTDI <sub>vol</sub> , DLP and effective dose from coronary CTA of 41 patients in 4 protocols of various heart rates.....	38
4.9 Patient protocol compared with other studies.....	40
4.10 Image noise.....	40
4.11 Overall image scoring.....	41
4.12 Image scoring in each protocol.....	42

## LIST OF FIGURES

<b>Figure</b>	<b>Page</b>
1.1 (a) CT images of the curved thin-slab maximum-intensity projection through the centerline of the RCA, LAD, and LCX. (b) CT volume-rendered image of RCA.....	1
2.1 Diagram of CT scanner (a) ‘End view’, (b) ‘Side view’.....	5
2.2 Multi slice CT scanner x-ray beam and detector (a) approximately to scale (b) schematic diagram.....	5
2.3 Technological advances in CT scanner, 1985-2000.....	7
2.4 Effect of detector array on number of rotations and scan time.....	8
2.5 (a) PMMA body phantom (b) illustration of CTDIvol.....	11
2.6 Automatic tube current control in CT (a) in different-sized patients, (b) along the patient’s long axis and (c) throughout a gantry rotation.....	12
2.7 Diagram shows the range of diastolic regions for varying heart rates.....	14
2.8 The prospective ECG-triggered scan mode.....	16
2.9 The retrospective ECG-gated scan mode.....	17
3.1 320 detector row CT Toshiba Aquilion ONE scanner.....	22
3.2 Cylindrical PMMA phantom of 16 and 32 cm-diameter phantom.....	23
3.3 Catphan® 600 phantom.....	24
3.4 Unfors model Xi platinum dosimeter.....	24
3.5 10 cm length of the pencil-type ionization Unfors Xi CT detector.....	25
4.1 CTDIvol (mGy) and CTDIw (mGy) of head phantom as the function of kVp are plotted in red and blue straight lines.....	35
4.2 CTDIvol(mGy) and CTDIw (mGy) of body phantom as the function of kVp are plotted in red and blue straight lines.....	36
4.3 Bar chart of the effective dose from 41 patients underwent coronary CTA..	39
4.4 Bar chart of the effective dose from 30 patients in PGT 70-80% 1RR.....	39
4.5 Bar chart of the effective dose from 3 patients in PGT 30-80% 1RR.....	40
4.6 Bar chart of the effective dose from 3 patients in PGT 30-80% 2RR.....	40
4.7 Bar chart of the effective dose from 5 patients in RGT with dose Modulation.....	40
4.8 Effective dose, mSv from 41 patients, underwent coronary CTA in 4 protocols were compared to other studies.....	41
4.9 Effective dose from 30 patients from PGT 70-80%1RR in 4 range of BMI.	42
4.10 Bar chart of image noise and the effective dose.....	43

## LIST OF ABBREVIATIONS

<b>Abbreviation</b>	<b>Terms</b>
MDCT	Multi-detector computed tomography
CAD	Coronary artery disease
CCTA	Coronary computed tomography angiography
RCA	Right coronary artery
LMA	Left main coronary artery
LAD	Left anterior descending artery
LCX	Left circumflex artery
CTDI	Computed Tomography Dose Index
DLP	Dose-Length Product
E	Effective dose
3D	Three dimensions
2D	Two dimensions
Lp/cm	Line pairs per cm
MTF	Modulation transfer function
FWHM	Full width at half maximum
cm	Centimeter
mm	Millimeter
mA	Milliamperere
mAs	Milliamperere-second
ms	Milli-second
ECG	Electrocardiography
mSv	Millisievert
CTDI <sub>vol</sub>	Volume computed tomography dose index
CTDI <sub>w</sub>	Weighted computed tomography dose index
PMMA	Polymethylmethacrylate
DRLs	Dose reference levels
PGT	Prospective gating technique
RGT	Retrospective gating technique
ml	Milliliter
mg	Milligram
kV	Kilo voltage
kVp	Kilo voltage peak
kW	Kilo watt
MHU	Mega heat unit
HR	Heart rate
FDA	Food and drug administration
g	Gram
μGy	Microgray
mGy	Milligray
mGy.cm	Milligray-centimeter
mR	Milliroentgen
kPa	Kilopascal
Cr	Creatinine
BMI	Body mass index
Kg/ m <sup>2</sup>	Kilogram per meter square

<b>Abbreviation</b>	<b>Terms</b>
ROI	Region of interest
SD	Standard deviation
bpm	Beat per minute
HU	Hounsfield unit
FOV	Field of view
N	Noise

# CHAPTER I

## INTRODUCTION

### 1.1 Background and rationale

Computed Tomography (CT) is a medical imaging modality which cross-sectional image of body has been obtained since its introduction into diagnostic radiology in early 1970s. Technical developments in CT result in the introduction of multi-detector computed tomography (MDCT) in 1999 [1]. MDCT is aiming to improve spatial resolution by decreased slice thickness and scan time, increase area of coverage by increasing detector rows and shortening tube rotation time. At present, the numbers of detector slices have been developed from 4, 16, 64, 128, 256 and 320. As the number of detector slice increases and with faster gantry rotation speed, the temporal resolution and spatial resolution improve leading to better cardiac imaging.

Coronary artery disease (CAD) is an important cause of mortality and morbidity worldwide. According to WHO estimation in 2004, 16.7 million people die of cardiovascular diseases each year [2]. Noninvasive method to evaluate the heart and its coronary arteries has long been desired by the medical community. CT is one of the best modality producing high spatial resolution image, fast scanning speed and adequate area of coverage. The coronary arteries have been visualized directly by Coronary Computed Tomographic Angiography (CCTA) as shown in figure.1.1. CCTA requires the injection of intravenous contrast medium to visualize the coronary arteries, to determine whether plaque is present, and if so, to determine the degree to which it narrows the artery. CCTA assesses for the presence and determines the severity of blockages of the arteries to the heart (coronary arteries). These blockages are due to fat and cholesterol ("plaques") that stick to the arterial wall and narrow the arteries. They are the principle cause of heart attack and sudden cardiac death. Severe blockade of the coronary arteries also causes chest pain and shortness of breath.

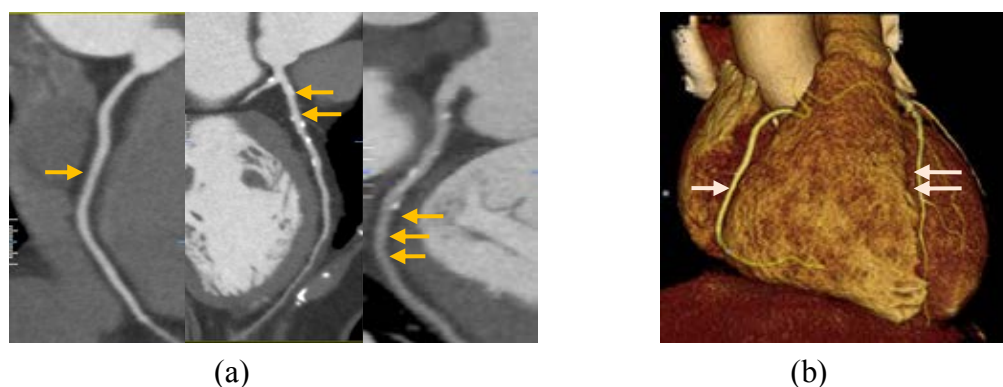


**Figure 1.1;** (a) CT images of the curved thin-slab maximum-intensity projections through the centerline of the right coronary artery (*RCA single arrow*), left anterior descending artery (*LAD double arrows*), and left circumflex artery (*LCX triple*

arrows). (b) CT volume-rendered image of RCA (*single arrow*) and LAD (*double arrows*).

Many studies [6], [8] have shown that the accuracy for detecting CAD by MDCT is high compared to conventional coronary angiography. MDCT scanners (seventh generation) offer the greatest degree of spatial and temporal resolutions owing to up to 320-detector channels, gantry rotation times of 0.35 seconds and collimation as narrow as 0.5 mm. These parameters are important to produce high definition coronary artery MDCT imaging and are invaluable in imaging of myocardial and valve function, pulmonary vein and aortic anatomy.

ECG gating enables acquisition of image data and image reconstruction at precise time points during the R-R interval. Image acquisition can occur throughout the R-R interval (retrospective gating) or at a predefined time point (prospective gating). In prospective gating, the radiation source is active only during a short segment of the R-R interval, optimally at 70 - 80% of the R-R interval when imaging the coronary arteries. Using retrospective gating, image data are acquired throughout several cardiac cycles and is subsequently divided into segments based upon the time lapsed from the beginning of each R-R interval. The first R wave is the 0% time point; each subsequent R wave is the 100% time point for the previous cardiac cycle and the 0% time point for the next R-R interval. The user defines the segment of image data which will be reviewed for diagnosis.

The radiation dose delivered to the patient is much higher using retrospective gating compared to prospective gating because the patient is exposed to radiation continually, throughout the scan. Each MDCT manufacturer has a method for dose reduction when using retrospective gating during the phases of the scan which are typically suboptimal for coronary artery imaging. So, the effective radiation dose from CCTA is an important factor for the awareness of the risk to the patient. Usually the patient dose in CT is expressed in terms of Computed Tomography Dose Index (CTDI) and Dose-Length Product (DLP) leading to the calculation of the effective dose.

## 1.2 Objective

To evaluate radiation dose and image quality of Coronary Computed Tomographic Angiography in 320-Detector Row Computed Tomography.

## 1.3 Definition

Multi-slice Detector Computed Tomography (MDCT)

CT scanner with detector array of more than single row of detectors that allows the simultaneous scanning of more than one slice.



Coronary artery disease (CAD)	The condition which plaque builds up inside the coronary arteries.
Coronary Computed Tomographic Angiography (CCTA)	Non invasive method to evaluate the coronary arteries by the use of Computed Tomography
Computed Tomography Dose Index (CTDI)	The equivalent of the dose value inside the irradiated slice that would result if the radiation dose profile were entirely concentrated to rectangular profile of width equal to the nominal slice thickness. Accordingly, all absorbed dose contributions from the nominal slice width, i.e. the areas under the tails of the dose profile, are added to the area inside the slice.
Dose-Length Product (DLP)	An indicator of the integrated radiation dose of an entire CT examination. The DLP incorporates the number of scans and the scan width (i.e., total scan length). The definition of DLP is: $DLP = CTDI_{vol} \times \text{Scan length}$ .
Effective dose (E)	The organ doses from a partial irradiation of the body are converted into an equivalent uniform dose to entire body.

## CHAPTER II

### REVIEW OF RELATED LITERATURES

#### 2.1 Theory

##### 2.1.1 The introduction of CT

X-ray computed tomography (CT) is a medical imaging method used to generate a three-dimensional image of the inside of an object from a large series of two-dimensional X-ray images taken around a single axis of rotation. They provide anatomical information by the principle that different types of tissues, depending on their composition and density, absorb varying amount of x-rays. CT produces a volume of data that can be manipulated, through a process known as "windowing", in order to demonstrate various bodily structures based on their ability to block the X-ray beam. Although historically the images generated were in the axial or transverse plane, orthogonal to the long axis of the body, modern scanners allow this volume of data to be reformatted in various planes or even as volumetric (3D) representations of structures.

CT was introduced clinically in the early 1970s [2]. Collimator both within the image plane and between planes provides significant scatter rejection, there by substantially improves the subject contrast. In addition, the reconstructed cross-sectional CT image eliminates nearly all the problem of overlapping anatomy; indeed, CT provided the first clinical tomographic image data that allows physicians to see the internal structure of a 3D object in cross section. CT's adoption of high efficiency, low noise detectors that could respond linearly over a broad range of transmission values, moreover, provides uniform sensitivity over a wide variety of tissue attenuations and body thickness; these detectors, together with the digital nature of CT data, allow retrospective visualization of any range of transmission values, through image processing, and provide optimal image density irrespective of exposure levels.

The basic components of CT scanner are an x-ray tube and arch of detectors, mounted on a gantry with a circular aperture (Figure 2.1a). Along the patient long axis, there are many rows of these arches of detectors, giving rise to the term multi-slice CT (MSCT) (Figure 2.2) or multidetector CT (MDCT). The extent of area coverage by the detector rows currently ranges from 12 mm to 160 mm in length (Figure 2.2b) depends on scanner model. The patient lies on an integral couch, the x-ray tube and detectors rotate, continuous monitoring the absorption of x-rays as their path through the body changes. Image data can be acquired in sequential mode or in helical mode (Figure 2.1b). In sequential mode sometime known as axial mode or step and shoot mode, the couch is stationary during each rotation, then steps through the gantry to the next position in order to acquire another set of data.

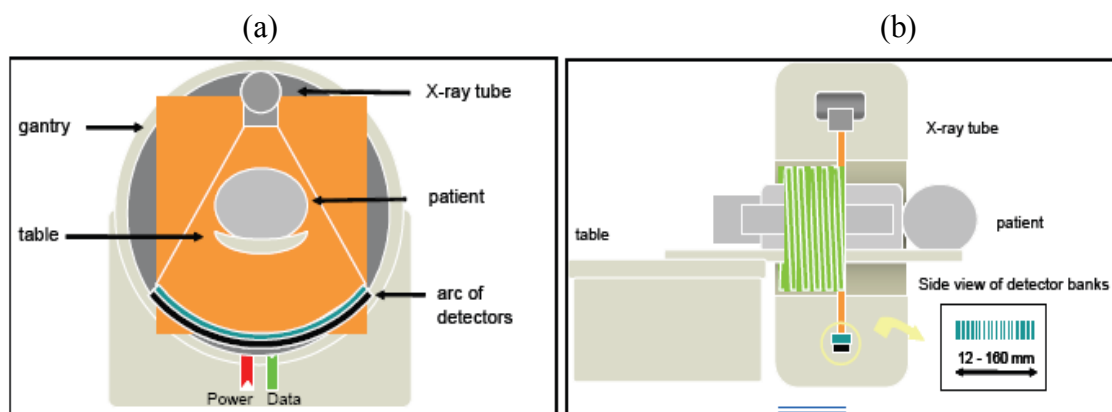


**Figure 2.1** Diagram of CT scanner (a) ‘End view’, (b) ‘Side view’ in helical acquisition mode

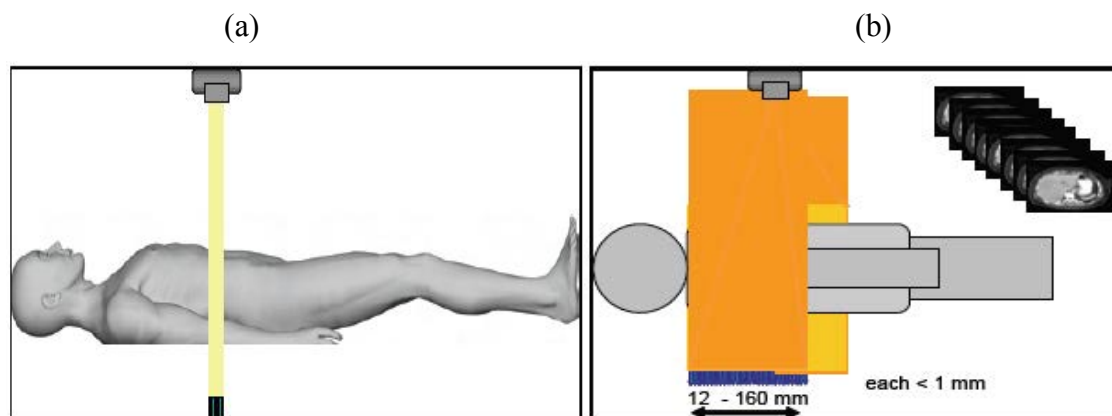


**Figure 2.2** CT scanner X ray beam and detector (a) approximately to scan  
(b) schematic diagram

### 2.1.2 Image Formation

The goal of x-ray CT is to determine the x-ray attenuation coefficients within a matrix of tissue volume elements, or voxels, within a plane of finite thickness. The attenuation coefficient at each voxel is reflected as the grayscale value of the corresponding pixel in the displayed 2D image of the slice. The numeric value assigned to a pixel corresponds to the average x-ray attenuation within its associated voxel, after normalization to the attenuation properties of water.

The slice’s pixel map is obtained from attenuation data generated by passing a large set of independent and very narrow x-ray beam through the object and measuring the amount of radiation transmitted for each. Each such transmission reading is a composite measure of the attenuation characteristics of all materials along the path of the x-ray beam. The cumulative attenuation along one x-ray path can be

expressed mathematically as the spatial line-integral of the appropriate attenuation coefficients.

The data are normalized to the initial x-ray intensity to form transmission values, to remove the dependence of the signal on initial beam intensity. After the log of transmission data is taken, the relevant signal can be approximated as ray-sum

$$\sum(\mu_i \times r_i) ,$$

where  $\mu_i$  is the linear attenuation coefficient of the material in the  $i^{th}$  voxel and  $\Delta r_i$  is the voxel's dimension along the x-ray path. A set of ray-sums across the width of a patient at a given projection angle is known as *projection*, or *view*. It is the set of projections at multiple angles that is mathematically reconstructed to form a 2D cross-sectional image of a thin 3D slice through the object.

A sinogram is another method of representing the data acquired in CT. It plots the transmitted x-ray signal magnitude according to the detector and x-ray tube positions and is typically displayed in terms of projection angle versus ray sum position within the projection.

### 2.1.3 Multiple Detector CT (MDCT)

To achieve more substantial volume coverage, faster and/or with improved z-axis resolution, are the concurrent acquisition of more than one slice, and a decrease in gantry rotation time. Beginning in 1998, CT manufacturers introduced 4-channel MDCT systems, which provided a considerable reduction in scan time, the ability to acquire thinner images with the same scan time, or more efficient utilization of the available x-ray beam. This began the current revolution in CT technology that has been the basis of a dramatic increase in the number and utility of CT clinical application. Two essential advances toward modern MDCT systems were the fabrication of x-ray detectors that were physically and electrically separated along the z-axis, and the ability to flexibly combine the data from the individual detector elements by assigning the output of more than one detector to a single data channel. The resulting decrease in scan time was of tremendous clinical advantage. At present, CT scanner has developed rapidly. Figure 2.3 illustrates the rapid pace of developments in scanner technology over the last twenty years, and especially the acceleration of development in last ten years from four to 320-slice scanner.

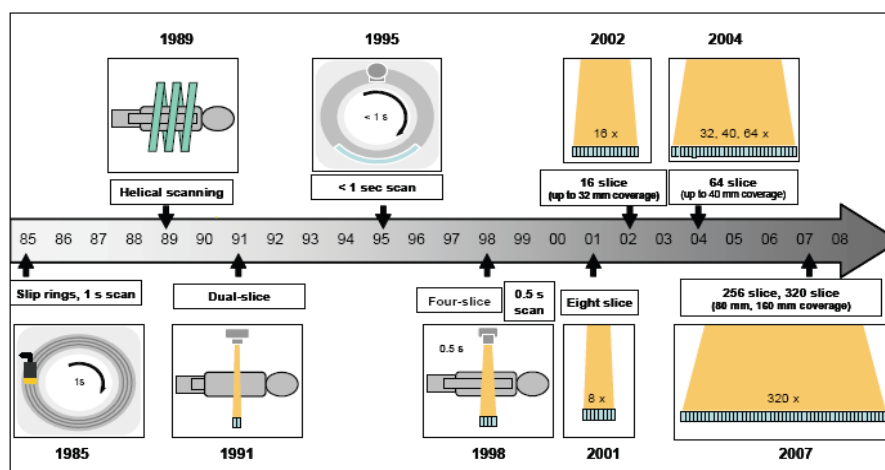


**Figure 2.3** Technological advances in CT scanner, 1985-2007

### 2.1.4 Scan time and scan length

The maximum scan length is an important factor in scanner performance, and may limit the ability to perform certain procedures, for example when scanning peripheral angiography run-off. Another aspect of maximum scan length that may need to be considered is the coverage available in dynamic studies such as CT perfusion scanning, where the same volume of patient is repeatedly scanned in quick succession. The maximum scan length is governed by the z-axis detector array design, and the x-ray tube heat characteristics. With the large volume of data generated with a 64 slice scanner, for example, the total scan length may also be limited by computer memory capacity.

#### 2.1.4.1 Gantry rotation time

The rotation time of the tube and the detectors around the patient (gantry rotation time) has a direct effect on total scan time. Image quality will be improved with faster rotation times, as there will be reduced misregistration of data (both in-plane and along the patient) arising from patient movement (whether from heart beat, breathing, peristalsis, or restlessness). This misregistration of data introduces artifacts in image.

Scanners can now achieve rotation times of less than 0.3 seconds, but the fastest rotations are generally reserved for specialist applications such as cardiac scanning in order to minimize image artifacts due to motion of heart.

#### 2.1.4.2 Detector array length

The length of detector array will determine the number of rotations needed to cover the total scan length, and thus the overall scan time. The example in figure 2.4 shows how the total scan time will be halved by doubling the array length. The ability to scan a given length with fewer rotations also helps to minimize heat load on the x-ray tube, thereby allowing the scanning of longer lengths.

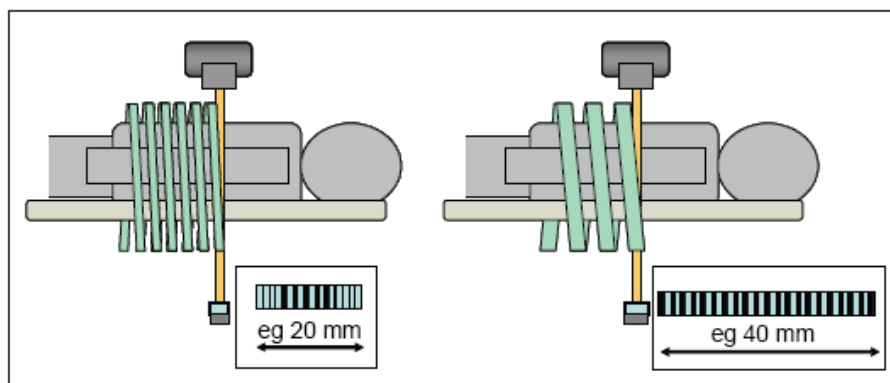


**Figure 2.4** Effect of detector array on number of rotations and scan time.

Detector arrays are divided into two types; fix and variable, or known as matrix and hybrid. Fixed arrays have detectors of equal z-axis dimension over the full extent of the array, whereas on variable arrays, the central portion comprises finer detectors. With variable arrays, the total scan time for a given length, the finest slice acquisition, will be longer, because the z-axis coverage is reduced.

Complete coverage of an organ, such as the brain or heart, offers advantages for both dynamic perfusion and cardiac studies. The z-axis detector array lengths on the 64-slice scanners, of up to 40 mm, are adequate to cover these organs in only few rotations. A coverage length of 160 mm usually allows complete organ coverage in a single rotation, so the function of the whole organ can be monitored over time.

### 2.1.5 Image quality

The principal parameters describing image quality are spatial resolution, contrast resolution, temporal resolution, and the prevalence of artifacts.

#### 2.1.5.1 Spatial resolution

Spatial resolution is the ability of the system to image an object without blurring. It is often described as the sharpness of an image. It may be quoted as the smallest object size able to be discerned, and as such is evaluated using high contrast test objects where signal to noise level is high and does not influence perception. It can also be specified in terms of spatial frequency, in line pairs per cm (lp/cm), for particular levels of the modulation transfer function (MTF); usually at the 50%, 10% and 2% or 0% levels. The 0% MTF level is referred to as the cut-off frequency and reflects the limit of the spatial resolution. The visual limit of spatial resolution, as the minimum size of high contrast objects, in millimeters, that can be distinguished, more generally relates to the frequency values between approximately the 2 and 5% modulation of the MTF. Sometimes a visual limited value is given by the manufacturers, either from a visual test object, or by converting the 2% value on the MTF to its size in mm.

The following scanner design features affect the x-y plane spatial resolution:

- Focal spot size (x-dimension)



- Focal spot stability
- Detector size (x-dimension)
- Number of 'views' per rotation (sampling frequency)
- 'Over-sampling' techniques
- Quarter-detector shift
- Flying/dynamic focal spot
- Attenuating grid (x-y plane)

The z-axis resolution is often referred to as z-sensitivity and is quoted in terms of the full width at half maximum (FWHM) of the imaged slice dose profile, but it may also be determined by the MTF. It is governed by similar factors as the x-y plane resolution:

- Focal spot size (z-dimension)
- Focal spot stability
- Detector size (z-dimension)
- 'Over-sampling' techniques
- Optimal pitch values
- Z-axis flying/dynamic focal spot
- Attenuating grid (z-axis)

The z-axis resolution is primarily determined by the z-axis detector dimensions. Z-axis detector array design on MDCT scanners varies considerably between systems, with minimum dimensions ranging from 0.50 to 0.75 mm. As described earlier, some arrays are fixed design, whilst others are a variable design. With variable arrays, the z-axis spatial resolution will be reduced when the full extent of the array is used for imaging, as data from adjacent detectors are combined, increasing the effective detector size.

#### **2.1.5.2 Contrast resolution**

Contrast resolution is the ability to resolve an object from its surroundings where the CT numbers are similar (*e.g.* in the imaging of liver metastases). It is sometimes referred to as low contrast resolution or low contrast detectability. The ability to detect an object will be dependent on its contrast, the level of image noise and its size. Contrast resolution is usually specified as the minimum size of object of a given contrast difference that can be resolved for a specified set of scan and reconstruction parameters.

Generator power is an important factor in low contrast examinations. Low noise images require high tube current (mA) values, particularly when coupled with fast rotation speeds and narrow slice acquisitions. Fast rotation speeds reduce movement artifacts, thin slices improve spatial resolution as well as reduce partial volume effects. Dose efficiency of the scanner is a significant factor in these types of examinations, as it will determine the dose required for a given level of contrast resolution. Contrast resolution specifications should give a guide to a scanner's dose efficiency. However, there is no standard methodology of data acquisition and image quality scoring to enable a good comparison of manufacturers' data.

### 2.1.5.3 Temporal resolution

In CT, temporal resolution is usually considered in the context of cardiac scanning. The aim, in cardiac CT, is to minimize image artifacts due to motion of the heart. This can be achieved using ECG-gating techniques, and imaging the heart during the period of least movement in the cardiac cycle, for a time interval of about 10% of the cycle. This results in a temporal resolution requirement of about 100 ms for a heart rate of 60 beats per minute. The temporal resolution is defined as the time taken to acquire a segment of data for image reconstruction. For 'single segment' reconstruction, it will be the time taken to acquire  $180^\circ$  of data, *i.e.* the time for half a gantry rotation. However, for higher heart rates this can still result in unacceptable cardiac motion artifacts. In this situation data from multiple, smaller segments, acquired from successive rotations, can be summed in order to obtain the  $180^\circ$  dataset. Using the multi-segment reconstruction approach requires an asynchrony between the gantry rotation and the patient's heart rate so that data from the successive segments are not acquired at the same angular positions.

### 2.1.5.4 Image artifacts

Artifacts are defined as structures in the image that are not present in the object. An imaging system will invariably produce some level of artifact, but it becomes an issue if it obscures an abnormality, resulting in a false negative diagnosis, or mimics an abnormality, giving a false positive result. Artifacts can be due to patient factors, scanner design factors or the reconstruction process, which by necessity involves some approximations. The sources of the image artifacts are:

- Patient motion
- Partial volume effect
- Photon starvation
- Metal objects
- Beam hardening
- Helical scanning
- Cone-beam geometry

For MDCT scanners, patient motion and partial volume artifacts will generally be reduced due to the decreased scan time and the ability to acquire with narrow slices. Photon starvation artifacts, *i.e.* streaks arising from the high attenuation in lateral projections of areas such as the shoulders and pelvis can be reduced with angular tube current modulation. Other artifacts, such as those resulting from the extended X-ray beam along the z-axis, will be increased. These are generally referred to as 'cone-beam' artifacts. Traditional back-projection methods of reconstruction in CT assume parallel-beam geometry in the y-z plane. As the z-axis beam extent is increased, this assumption breaks down and 'cone-beam' reconstruction methods must be used to avoid excessive artifacts. Some manufacturers employ adaptations of the back-projection approach, whereas others use 3D methods such as approximations of the Feldkamp reconstruction. Although 3D methods are more exact, they may require longer reconstruction time. Cone-beam reconstructions are generally only implemented in helical scanning, therefore in sequential scanning, the extent of beam used, or the narrow slice reconstructions, may be limited. The latest scanners, with

beam extents of 80 mm to 160 mm, by necessity also use cone-beam reconstruction methods in sequential scan mode.

### 2.1.6 Ionizing radiation and patient dose

Doses from CT examinations are generally significantly higher than those from conventional X-rays, although a CT scan provides more diagnostic information. Recent UK surveys[2] reported conventional X-ray examinations with average doses of 0.04 mSv for head examinations, 0.02 mSv for chest and 0.7 mSv for abdomen examinations. A similar survey for CT examinations gave values of 1.5, 5, and 6 mSv respectively for the head, chest and abdomen regions [4]. These figures represent average values from the use of a wide range of operational parameters, such as tube current and voltage, however they can be used as a guide.

The standard reference parameters used to describe dose in CT are the CTDI<sub>vol</sub> (volume computed tomography dose index) and the DLP (dose length product). The CTDI<sub>vol</sub> is calculated from measurements, made with a 100mm long pencil ion chamber, in standard sized polymethylmethacrylate (PMMA) head and body phantoms which have been irradiated at the halfway position, along the length, with a single beam rotation. However, as a dose descriptor, it is important to think of the CTDI<sub>vol</sub> as representing the average dose in a slice of tissue, halfway along a 100 mm irradiated length. The DLP represents the total amount of irradiation given, and as such gives an indicator of risk (without taking into account the radiosensitivity of particular organs). The CTDI<sub>vol</sub> is a very useful dose descriptor for comparing dose from different protocols or different scanners. However, comparisons should only be done for scans undertaken on standard size patients.

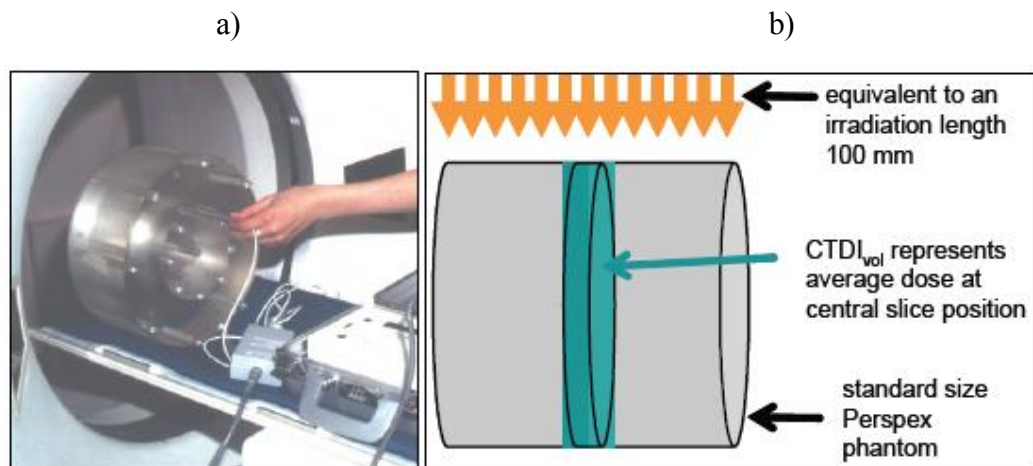


**Figure 2.5** a) PMMA body phantom used for measurement of CT doses b) illustration of CTDI<sub>vol</sub> representing average dose at central slice position of 100mm irradiation length

The CTDI<sub>vol</sub> and sometimes the DLP values are displayed on the scanner console. It is always invaluable to look at these figures when reviewing patient images for an assessment of the image quality and dose performance of a scanner. Both the CTDI<sub>vol</sub> and the DLP are used when comparing with dose reference levels (DRLs).

MDCT scanners have the potential to give higher radiation doses compared to single slice scanners. Their flexibility in scanning lengths with high mAs values, and the ease with which they perform dual and even triple-phase contrast studies, can lead to high patient doses. In addition, there are some intrinsic features of current MDCT design which can give rise to slightly higher doses.

### 2.1.7 Automatic tube current control in CT

Traditionally, the X-ray tube current (mA) in CT was selected for a particular protocol, and remained constant throughout a scan. Any changes to accommodate different sized patients had to be estimated and implemented manually. Modern scanners are equipped with automatic exposure control mechanisms, which adjust the tube current for changing patient attenuation throughout a scan. The adjustment can be made to compensate for changing attenuation (Figure 2.6) Most modern systems have the capability to operate all three compensation modes, which are generally implemented simultaneously. Most scanners will allow manual de-selection of one or more modes, and on others the de-selection may be implemented automatically within a protocol, according to the clinical region scanned.

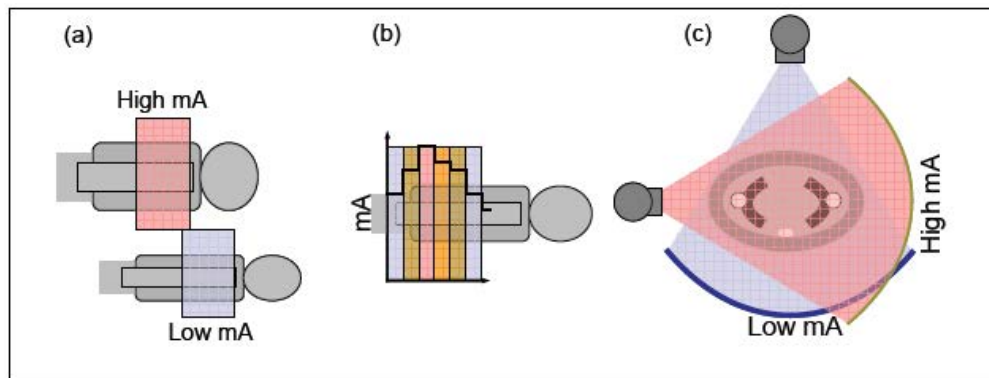


**Figure 2.6** Automatic tube current control in CT (a) in different-sized patients; (b) along the patient's long axis; and (c) throughout a gantry rotation.

### 2.1.8 Cardiac scanning

The prospect of imaging the heart and coronary arteries with CT has been anticipated since the development of CT more than 3 decades. The lack of speed and poor spatial and temporal resolutions of previous generations of CT scanners prevented meaningful evaluation of the coronary arteries and cardiac function. Most early assessments of the coronary arteries with CT were performed with electron beam CT, developed in the early 1980s. Electron beam CT has been used mostly for noninvasive evaluation of coronary artery calcium, but other applications including assessment of coronary artery stenosis have been reported in limited cases. However, electron beam CT is expensive and not widely available. Recent advances in CT technologies, especially multiple-row detector CT, have dramatically changed the approach to noninvasive imaging of cardiac disease. With sub millimeter spatial resolution ( $<0.75$  mm), improved temporal resolution (80–200 msec) [5], and

electrocardiographically (ECG) gated or triggered mode of acquisition, the current generation of CT scanner makes cardiac imaging possible and has the potential to accurately characterize the coronary tree. The factors affecting temporal and spatial resolution are scan acquisition and reconstruction methods, reconstruction algorithms, reconstruction interval, pitch, radiation dose, and geometric efficiency.

In order to image a rapidly beating heart, the imaging modality should provide high temporal resolution. It is necessary to freeze the heart motion in order to image coronary arteries located close to heart muscles, since these muscles show rapid movement during the cardiac cycle. Since the most quiescent part of the heart cycle is the diastolic phase, imaging is best if performed during this phase. Hence, it is required to monitor the heart cycle during data acquisition. The subject's electrocardiogram (ECG) is recorded during scanning because the image acquisition and reconstruction are synchronized with the heart motion. Also, the imaging modality should provide high spatial resolution to resolve very fine structures such as proximal coronary segments (right coronary and left anterior descending arteries) that run in all directions around the heart. These requirements impose greater demands on multiple-row detector CT technology. One of the primary goals of the rapid development of CT technology has been to achieve these demands in order to make cardiac CT imaging a clinical reality.

To better demonstrate and understand the necessity for high temporal resolution in cardiac imaging, Figure 2.7 shows how the length (in time) of the diastolic phase changes with heart rates. The least amount of cardiac motion is observed during the diastolic phase; however, the diastolic phase narrows with increasing heart rate. With rapid heart rates, the diastolic phase narrows to such an extent that the temporal resolution needed to image such subjects is less than 100 msec. The desired temporal resolution for motion-free cardiac imaging is 250 ms for heart rates up to 70 beats per minute and up to 150 ms for heart rates greater than 100 beats per minute. Ideally, motion-free imaging for all phases requires temporal resolution to be around 50 msec. The standard of reference for comparing the temporal resolution obtained with multiple-row detector CT is fluoroscopy, wherein the heart motion is frozen during dynamic imaging to a few milliseconds (1–10 ms). Therefore, the demand for high temporal resolution implies decreased scan time required to obtain data needed for image reconstruction and is usually expressed in milliseconds.

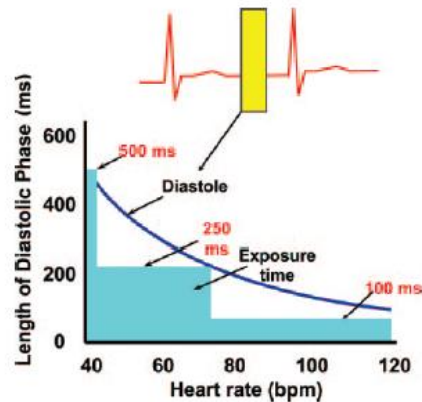


**Figure 2.7** Diagram shows the range of diastolic regions for varying heart rates. The desired temporal resolution for cardiac CT is approximately 250 ms for average heart rates of less than 70 beats per minute; for higher heart rates, the desired temporal resolution is approximately 100 ms.

The demand for high spatial resolution that enables the visualization of various coronary segments (such as the right coronary artery, left anterior descending artery, and circumflex artery) that run in all directions around the heart with decreasing diameter is high. These coronary segments range from a few millimeters in diameter (at the origins) and decrease to a few sub millimeters in diameter as they traverse away from the aorta in all directions. The need to image such small coronary segments requires small voxels, and this is a key to cardiac imaging with multiple-row detector CT. Spatial resolution is generally expressed in line pairs per centimeter or line pairs per millimeter. Like temporal resolution, the standard of reference for comparing spatial resolution is the resolution obtained during fluoroscopy. However, one of the major goals of multiple-row detector CT technology development has been to obtain similar spatial resolution in all directions, also expressed as isotropic spatial resolution.

In addition, a sufficient contrast-to-noise ratio is required to resolve small and low contrast structures such as plaques. In CT, low-contrast resolution is typically excellent. However, it can be degraded with the increasing number of CT detectors in the z direction due to increased scattered radiation that can reach detectors in the z direction. It is important to achieve adequate low-contrast resolution with minimum radiation exposure. The need to keep radiation dose as low as reasonably possible is essential for any imaging modality that uses ionizing radiation. Overall, cardiac imaging is a very demanding application for multiple-row detector CT. Temporal, spatial, and contrast resolution must all be optimized with an emphasis on minimizing radiation exposure during cardiac CT imaging.

### 2.1.9 Factors influenced the temporal resolution

There are a number of factors that influence the temporal resolution achieved with MDCT scanners. Among them, the key factors are the gantry rotation time, acquisition mode, type of image reconstruction, and pitch.



### 2.1.10 Gantry Rotation Time

Gantry rotation time is defined as the amount of time required to complete one full rotation ( $360^\circ$ ) of the x-ray tube and detector around the subject. The advances in technology have considerably decreased the gantry rotation time to as low as 330–370 ms. The optimal temporal resolution during cardiac imaging is limited by the gantry rotation time. The faster the gantry rotation, the greater the temporal resolution achieved. However, with increasing gantry rotation speed, there is also an increase in the stresses on the gantry structure, since rapid movement of heavy mechanical components inside the CT gantry results in higher G forces, making it harder to achieve a further reduction in gantry rotation time. In fact, even a small incremental gain in the gantry rotation time requires great effort in the engineering design. In the past, the minimum rotation time was as high as 2 seconds; in the past few years, gantry rotation time has decreased steadily to less than 400 msec. As discussed in the previous section and in Figure 2.7, since the currently available gantry rotation time is not in the desired range for obtaining reasonable temporal resolution, various methods have been developed to compensate, such as different types of scan acquisitions or image reconstructions to further improve temporal resolution.

### 2.1.11 Acquisition Mode

For imaging the rapidly moving heart, projection data must be acquired as fast as possible in order to freeze the heart motion. This is achieved in MDCT either by prospective ECG triggering or by retrospective ECG gating.

**2.1.11.1 Prospective ECG Triggering.**—This is similar to the conventional CT “step and shoot” method. The patient’s cardiac functions are monitored through ECG signals continuously during the scan. The CT technologist sets up the subject with ECG monitors and starts the scan. Instructions are built into the protocol to start the x-rays at a desired distance from the R-R peak, for example at 60% or 70% of the R-R interval. The scanner, in congruence with the patient’s ECG pulse, starts the scan at the preset point in the R-R interval period (Fig 2.8). The projection data are acquired for only part of the complete gantry rotation (i.e., a partial scan).

The minimum amount of projection data required to construct a complete CT image is  $180^\circ$  plus the fan angle of the CT detectors in the axial plane. Hence, the scan acquisition time depends on the gantry rotation time. The best temporal resolution that can be achieved in the partial scan mode of acquisition is slightly greater than half of the gantry rotation time. Once the desired data are acquired, the table is translated to the next bed position and, after a suitable and steady heart rate is achieved, the scanner acquires more projections. This cycle repeats until the entire scan length is covered, typically 12–15 cm (depending on the size of the heart).

With MDCT, the increasing number of detectors in the z direction allows a larger volume of the heart to be covered per gantry rotation. This has a major advantage in terms of the decreased time required for breath holding to minimize motion artifacts (critical when scanning sick patients). One of the advantages of the prospective triggering approach is reduced radiation exposure, because the projection data are acquired for short periods and not throughout the heart cycle.

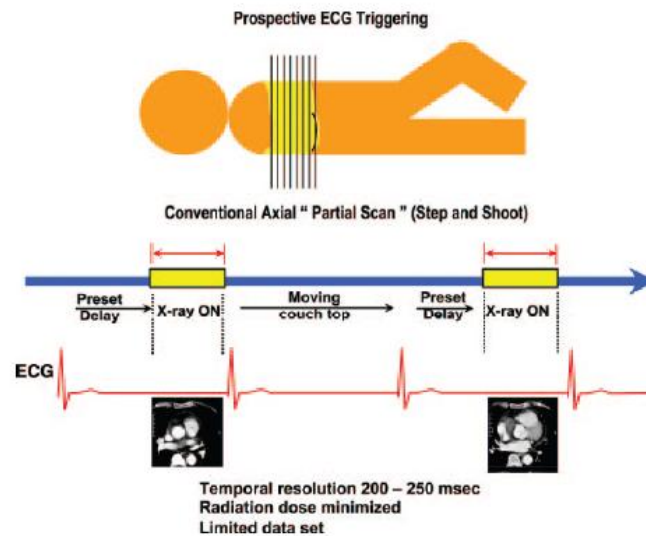


**Figure 2.8** During the prospective ECG-triggered scan mode, the patient's ECG is continuously monitored but the x-rays are turned on at predetermined R-R intervals to acquire sufficient scan data for image reconstruction. The table is then moved to the next location for further data acquisition. These types of scans are always sequential and not helical and result in a lower patient dose because the x-rays are on for a limited period. Calcium scoring scans are typically performed in this scan mode.

**2.1.11.2 Retrospective ECG Gating.**—Retrospective gating is the main choice of data acquisition in cardiac coronary artery imaging with MDCT. In this mode, the subject's ECG signals are monitored continuously and the CT scan is acquired continuously (simultaneously) in helical mode (Fig 2.8). Both the scan projection data and the ECG signals are recorded. The information about the subject's heart cycle is then used during image reconstruction, which is performed retrospectively, hence the name *retrospective gating*. The image reconstruction is performed either with data corresponding to partial scan data or with segmented reconstruction.

The disadvantage of the retrospective gating mode of acquisition is the increased radiation dose, because the data are acquired throughout the heart cycle, even though partial data are actually used in the final image reconstruction. Also, since this scan is performed helically, the tissue overlap specified by the pitch factor is quite low, indicating excessive tissue overlap during scanning, which also increases radiation dose to the patients. The need for low pitch values or excessive overlap is determined by the need to have minimal data gaps in the scan projection data required for image reconstruction. The need for low pitch values is discussed in detail in the section on pitch.

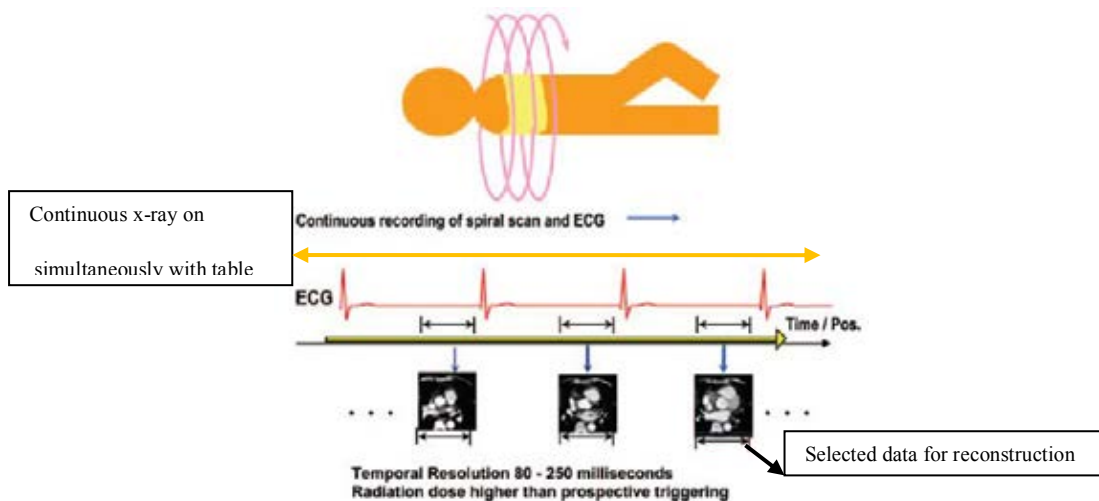


**Figure 2.9** During the retrospective ECG-gated scan mode, the patient's ECG is continuously monitored and the patient table moves through the gantry. The x-rays are on continuously, and the scan data are collected throughout the heart cycle. Retrospectively, projection data from select points within the R-R interval are selected for image reconstruction.

### 2.1.12 Reconstruction Method

Cardiac data acquired with either prospective ECG triggering or retrospective ECG gating are used in reconstructing images. High temporal resolution images are obtained by reconstructing the data either with partial scan reconstruction or with multiple-segment reconstruction.

**2.1.12.1 Partial Scan Reconstruction.**—among the methods of image reconstruction in cardiac CT, the most practical solution is the partial scan reconstruction. Partial scan reconstruction can be used for both prospective triggering and retrospective gating acquisitions. The minimum amount of data required to reconstruct a CT image is at least  $180^\circ$  plus the fan angle of data in any axial plane. This determines the scan time to acquire projection data needed for partial scan reconstruction and also limits the temporal resolution that can be achieved from an acquisition. The CT detectors in the axial plane of acquisition extend in an arc that covers at least a  $30^\circ$ – $60^\circ$  fan angle. Therefore, during partial scan reconstruction, the scan data needed for reconstruction are obtained by rotating the x-ray tube by  $180^\circ$  plus the fan angle of the CT detector assembly.

**2.1.12.2 Multiple-Segment Reconstruction.**—the primary limitation to achieving high temporal resolution with the partial scan approach is the gantry rotation time. To achieve even higher temporal resolution, multiple-segment reconstruction was developed. The principle behind multiple segment reconstruction is that the scan projection data required to perform a partial scan reconstruction are selected from various sequential heart cycles instead of from a single heart cycle. This is possible only with a retrospective gating technique and a regular heart rhythm. The CT projection data are acquired continuously throughout many sequential heart cycles.

### 2.1.13 Spatial Resolution

There are a number of factors that influence the spatial resolution achieved with MDCT scanners. Among them are the detector size in the longitudinal direction, reconstruction algorithms, and patient motion.

Cardiac imaging is a highly demanding application of multiple-row detector CT and is possible only due to recent technological advances. Understanding the trade-offs between various scan parameters that affect image quality is key in optimizing protocols that can reduce patient dose. Benefits from an optimized cardiac CT protocol can minimize the radiation risks associated with these cardiac scans. Cardiac CT has the potential to become a reliable tool for noninvasive diagnosis and prevention of cardiac and coronary artery disease.

## 2.2 Review of Related Literature

Many researchers studied the CT radiation dose in coronary computed tomography. Hausleiter J et al. [7] estimated radiation dose in 1,035 patients underwent coronary CTA. Scanning algorithms with and without an ECG-dependent dose modulation and with a reduced tube voltage were investigated on dose estimates and image quality. In the entire patient cohort, the effective doses were  $6.4 \pm 1.9$  and  $11.0 \pm 4.1$  mSv for 16- and 64-slice CTA, respectively ( $p < 0.01$ ). The reduction in radiation dose estimates ranged between 37-40% and between 53-64% with the use of ECG -dependent dose modulation and with the combined use of the dose modulation and reduced tube voltage, respectively. The reduction in dose estimates was not associated with a reduction in diagnostic image quality as assessed by signal-to-noise ratio and by the frequency of coronary segments with diagnostic image quality. The improvement in spatial and temporal resolution with 64 slice CTA resulted in increased radiation dose for coronary CTA.

Chen LK et al [9] studied in 50 patients for cardiac CT examination. All CCTA examinations were performed on a 256-slice CT scanner with one of five different protocols :retrospective ECG-gating (RGH) with full dose exposure in all R–R intervals (protocol A), RGH of 30–80% pulsing window with tube current modulation (B), RGH of  $78 \pm 5\%$  pulsing window with tube current modulation (C), prospective ECG-triggering (PGT) of 78% R–R interval with 5% padding window (D) and PGT of 78% R–R interval without padding window (E). Radiation dose parameters and image quality scoring were determined and compared. In this study, no significant differences were found in comparison on image quality of the five different protocols. Protocol A obtained the highest radiation dose when comparing with those of protocols B, C, D and E by a factor of 1.6, 2.4, 2.5 and 4.3, respectively ( $p < 0.001$ ), which were ranged between 2.7 and 11.8 mSv. The PGT could significantly reduce radiation dose delivered to patients, as compared to the RGH.

Duarte R et al [10] compared radiation dose and image quality parameters of CCTA between retrospective 64-MDCT and prospective 128-MDCT. A series of 77 consecutive patients were first randomized to either retrospective 64-MDCT ( $n = 37$ ) or prospective 128-MDCT ( $n = 40$ ) for CCTA. No significant differences were found regarding sex, age, bodyweight and heart rate. CCTA effective radiation dose was  $2.1 \pm 0.9$  vs.  $8.2 \pm 4$  mSv in prospective and retrospective ECG-gating MDCT groups, respectively. Mean image quality score was  $2.2 \pm 0.9$  for prospective 128-MDCT group and  $1.4 \pm 0.7$  points for retrospective 64-MDCT representing a mean difference of 0.8 points (CI: 0.9 to 0.7). In selected patients, CCTA using a 128-MDCT with prospective ECG-gating provides higher image quality with significant lower radiation dose when compared to 64-MDCT using retrospective ECG-gating.

Nasis A et al [6] studied diagnostic accuracy of noninvasive coronary angiography using 320-detector row computed tomography, which provide 16-cm craniocaudal coverage in 350 ms and image the entire coronary tree in a single heartbeat, representing a significant advance from previous generation scanners. They evaluated 63 consecutive patients who underwent 320-detector row computed tomography and invasive coronary angiography for the investigation of suspected coronary artery disease. All available coronary segments were included in the analysis, regardless of size or image quality. Lesions with  $>50\%$  diameter stenoses were considered significant. Mean heart rate was  $63 \pm 7$  beats/min, with 6 patients (10%) in atrial fibrillation during image acquisition. Thirty-three patients (52%) and 70 of 973 segments (7%) had significant coronary stenoses on invasive coronary angiogram. Seventeen segments (2%) were nondiagnostic on computed tomogram and were assumed to contain significant stenoses on an "intention-to-diagnose" analysis. Sensitivity, specificity, and positive and negative predictive values of computed tomography for detecting significant stenoses were 94%, 87%, 88% and 93%, respectively, by patient ( $n = 63$ ), 89%, 95%, 82%, and 97%, respectively, by artery ( $n = 260$ ), and 87%, 97%, 73%, and 99%, respectively, by segment ( $n = 973$ ). Overall median effective radiation dose was 10.6 mSv (interquartile range 8.0 to 13.8), comprising 5.4 mSv (interquartile range 4.4 to 6.3) for prospectively electrocardiographically triggered scans, 12.4 mSv (interquartile range 9.8 to 14.5) for retrospectively electrocardiographically triggered scans, 9.6 mSv (interquartile range 7.1 to 11.3) for single-beat acquisition scans and 14.2 mSv (interquartile range 9.3 to 15.0) for multibeat acquisition scans. In conclusion, noninvasive 320-detector row CT coronary angiography provides high diagnostic accuracy across all coronary segments, cardiac rhythm, or image quality.

Rybicki FJ et al [11] evaluated image quality and contrast opacification from 320-detector row CT. Patient dose is estimated for prospective and retrospective ECG-gating; initial correlation between 320-slice CT and coronary catheterization is illustrated. Retrospective image evaluation from forty consecutive patients included subjective assessment of image quality and contrast opacification (80 ml iopamidol 370 mg I/ml followed by 40 ml saline). CT findings were correlated from coronary catheterization. Estimated effective dose was compared for prospective versus

retrospective ECG-gating. For the most common (n=25) protocol (120 kV, 400 mA, prospective ECG-gating, 60-100% phase window, 16 cm craniocaudal coverage, single heartbeat, the mean dose was  $6.8 \pm 1.4$  mSv. Over 89% of arterial segments had excellent image quality. In conclusion initial 320-detector row coronary CT images have consistently excellent quality with iodinated contrast opacification.

Hoe J and Toh KH et al [12] assessed the effective radiation dose of MDCT with a 320-row detector volume scanner. Two hundred patients underwent cardiac scanning (110 kVp, n=9 or 120 kVp, n = 191; range 300-580 mA). Effective dose was estimated from extended dose length product. For heart rates (HRs) < 65 bpm, exposure phase was 65% up to end of R-R interval, using one beat acquisition. HRs from 66 to 79 bpm and > 80 bpm were scanned with either 2 or 3 heart beat acquisition, respectively. The mean effective dose was  $5.7 \pm 1.7$  mSv for 151 patients scanned with one heart beat acquisition. Qualitative image quality was assessed to be in good to excellent range, and mottle image quality was in low to medium mottle range. For patients scanned 2 or 3 heart beat acquisition, radiation dose was higher with mean exposures of  $13.0 \pm 3.3$  mSv and  $19.5 \pm 5.3$  mSv, respectively.



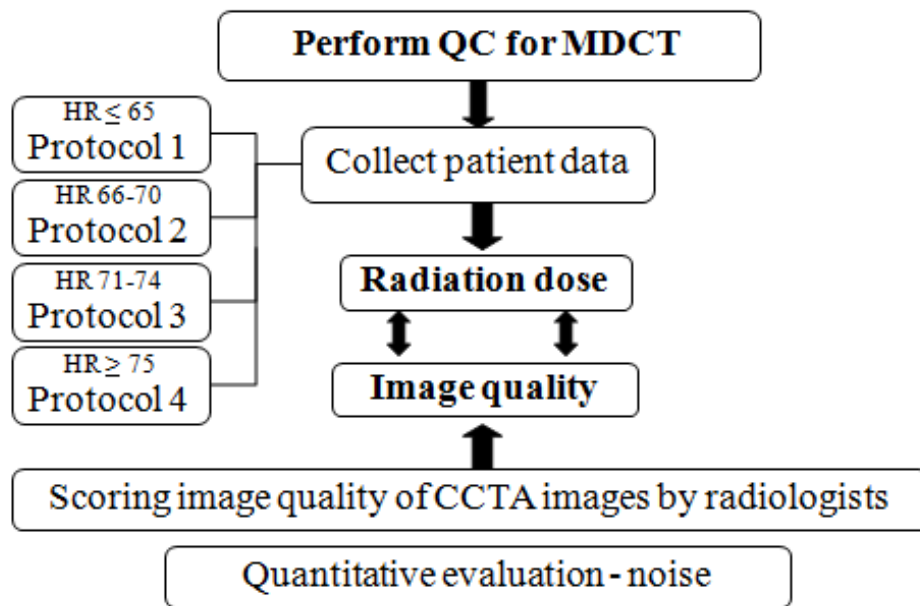
# CHAPTER III

## RESEARCH METHODOLOGY

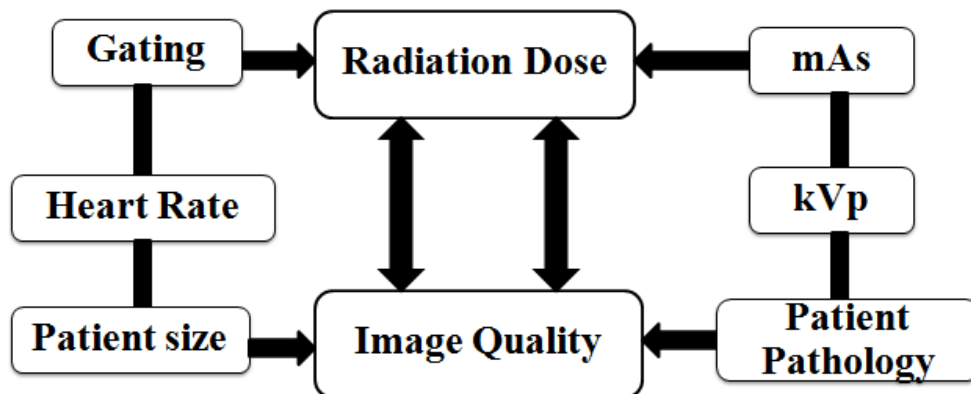
### 3.1 Research Design

This study is an observational descriptive design.

### 3.2 Research Design Model



### 3.3 Conceptual framework



### 3.4 Key words

- Effective dose
- Noise

### 3.5 Research question

What are the radiation dose and image quality of Coronary Computed Tomographic Angiography in 320-Detector Row Computed Tomography?

### 3.6 Materials

#### 3.6.1 CT scanner: Toshiba Aquilion ONE



**Figure 3.1** 320 detector row CT Toshiba Aquilion ONE scanner

In this study, CT scanner: 320-detector row CT Toshiba Aquilion ONE at Department of Radiology, King Chulalongkorn Memorial Hospital had been used. Computer software consists of operating system Window NT and the application software, coneXact™, used for acquisition and processing. CT scanner was installed in January 2011. The Toshiba Aquilion ONE is the third-generation multi-detector CT scanner, featuring a 70 kW generator, 7.5 MHU x-ray tube and fastest gantry rotation time of 0.35 seconds. It is capable of imaging 320 slices per rotation, with slice width of 320 x 0.5 mm and up to 640 slices per rotation by reconstruction.

#### 3.6.2 CT Phantom

The CT phantom is used to perform QC for CT system. The CT phantom is manufactured to comply with the FDA's performance standard for diagnostic x-ray systems. The cylindrical phantom consists of two 14 cm length made of solid

Polymethyl Methacrylate (PMMA) disks measuring 16 cm (head) and 32 cm (body) in diameter as shown in figure 3.2

There are 9 holes with acrylic rods to plug the holes for both phantoms when they are not used. Through holes are 1.31 cm in diameter and 14 cm length to accommodate standard CT probes. One is at center and four are around the perimeter, 90° apart and 1 cm hole center to the outside edge of each phantom.

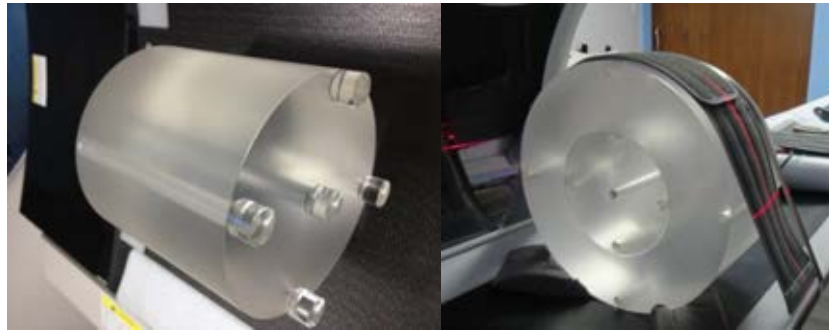


**Figure 3.2** Cylindrical PMMA phantom of 16 and 32 cm diameters

### 3.6.3 Catphan<sup>®</sup> 600 phantom

Catphan<sup>®</sup> 600 phantom was used for the performance study of the CT scanner as shown in Figure 3.3. The Catphan<sup>®</sup> phantom was positioned in the CT scanner by mounting on the case placed directly at the end of the table.

The Catphan<sup>®</sup> 600 phantom is all test sections located by precisely indexing the table from center of section 1 (CTP404) to the center of each subsequent test module. The indexing distances from section 1 are Catphan<sup>®</sup> 600 test module locations:

Module	Distance from section
1 center	
CTP404, slice width, sensitometry and pixel size	
CTP591, Bead geometry	32.5 mm
CTP528, 21 line pair high resolution	70 mm
CTP528, Point source	80 mm
CTP515, Subslice and supra-slice low contrast	110 mm
CTP486, Solid image uniformity module	150 mm

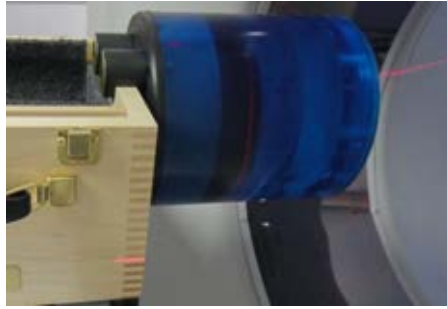


**Figure 3.3** Catphan<sup>®</sup> 600 Phantom. (The phantom laboratory, Catphan<sup>®</sup> 500 and 600 Manual, copyright© 2010)

### 3.6.4 Unfors model Xi platinum dosimeter

The Unfors Xi platinum (Figure 3.4) is a complete system for multi-parameter measurements on all modalities. The detector is solid state type which is not affected by the temperature and pressure of the environment. The system can be used for the calibration of the radiographic-fluoroscopic, mammography, dental and CT systems with an added option for luminance and illuminance measurements of medical monitors. The Unfors Xi platinum prestige is the ultimate QA solution fitted into a small and portable aluminum case. All Unfors Xi detectors are interchangeable and function with any base unit.

### 3.6.5 CT pencil-type ionization chamber

CT pencil-type ionization chamber of 4.9 cm<sup>3</sup> active volume, 10 cm total active length is shown in Fig3.5. The Unfors Xi CT detector is a new hybrid ion chamber designed by Unfors. The ion chamber and electronics are combined into one unit making it possible to measure both temperature and pressure to actively compensate for this dependency. The temperature is actually measured inside the ion chamber giving very precise compensations both with and without a CT phantom. With no baseline drift, this carbon fiber ion chamber is ready to use within one minute.



**Figure 3.4** Unfors model Xi platinum dosimeter



**Figure 3.5** 10 cm length of the pencil-type ionization Unfors Xi CT Detector

**Table 3.1** Characteristics of Unfors model Xi platinum dosimeter

Unfors Xi CT detector	
Unfors Xi base unit firmware	4.0 or higher
Size detector	200 x 20 x 12 mm (7.9 x 0.8 x 0.5 in)
Size diameter detector	7.5 mm (0.30 in)
Size diameter phantom adapter	12.5 mm (0.49 in)
Effective length	100 mm (3.94 in)
Weight	50 g (1.75 oz)
Range	10 $\mu$ Gy – 9999 Gy (1 mR – 9999R) 20 $\mu$ Gy/s – 100 mGy/s (140 mR/min – 680 R/min)
Uncertainty	5% (at 80 kV-150 kV; RQR and RQA qualities)
Radial uniformity	$\pm$ 2%
Axial uniformity	$\pm$ 3%, within rated length
Influence of relative humidity	< 0.3% (for RH < 80%)Uncertainty in temp. and pressure correction 2%
Pressure range	80.0 – 106.0 kPa
International standard	Fulfill requirements in IEC 61674

### 3.6.6 Patients

Patients underwent coronary computed tomography angiographic examination at Department of Radiology, King Chulalongkorn Memorial Hospital. Patients with previous allergic reaction to iodinated CM, hemodynamic instability, pregnancy and Cr > 1.5 mg/dL were excluded.

## 3.7 Methods

### 3.7.1 Perform the quality control of Toshiba Aquilion ONE

The quality control of CT scanner was performed following the AAPM report No.39 (1993): specification and acceptance testing of CT scanner [13] in the part of performance evaluation and ImPACT information leaflet 1: CT scanner acceptance testing version 1.02 [14]. The quality control program consists of the test of performance of electromechanical components, image quality and radiation dose.

### 3.7.2 Verification of CTDIvol and DLP

The CTDIvol and DLP are displayed on the monitor of the console of 320-detector row Toshiba Aquilion ONE. To make a confidence of using these values, the verification of CTDIvol and DLP were performed.

- Insert the pencil ionization chamber in the 16 and 32 cm diameter of PMMA phantom. The positioning of the phantom and chamber were investigated to avoid the alignment errors.
- Computed Tomography Dose Index (CTDI) and Dose Length Product (DLP) were recorded where the chamber is inserted at the center and the peripheral positions in phantom. The phantom was scanned three times for each kVp setting.
- The acquisition parameters were 2 x 4.0 mm. collimation, 1 sec rotation time and effective mAs 100. The CTDIvol and DLP that displayed on CT console were recorded.
- The data shown on dosimeter was recorded for the calculation of CTDIvol and compared to the displayed data on CT monitor.

### 3.7.3 Coronary CTA in the studied patients

Coronary CTA was performed in the patients with suspected coronary heart disease at King Chulalongkorn Memorial Hospital. The patients who are previous allergic to iodinated contrast media, hemodynamic instability, pregnancy and Cr > 1.5 mg/dL were excluded. The patients were scanned using various protocols based on their heart rate

HR  $\leq$  65    Protocol 1: Prospective gating 70-80% of R-R    (1 heart beat)

HR 66 – 70 Protocol 2: Prospective gating 30 -80 % R-R (1 heart beat)

HR 71 - 74 Protocol 3: Prospective gating 30 -80 % R-R (2 heart beat)

HR  $\geq$  75 Protocol 4: Retrospective with dose modulation

Before CCTA examination, if the patient's initial heart rate  $>$  65 bpm, beta blocker (metoprolol) was given 1 hour prior to the scanning. The mA and kVp were set according to the BMI of the patients.

**Table 3.2** mA and kVp setting

BMI(kg/m <sup>2</sup> )	kVp	mA
$\leq$ 20	120	300
21-25	120	350
26-30	120	400
$>$ 31	120	500

### 3.7.4 Data recording

Record the patient's information, scanning parameters, CTDIvol and DLP in case record form.

### 3.7.5 Evaluate the qualitative image quality

Evaluate the image quality by two radiologists independently using image quality criteria guideline from review of literature [10].

- Score 4 = excellent  
(Good vessel opacification with continuous course, without any motion artifacts)
- Score 3 = good  
(Good vessel opacification, minor motion artifacts or discrete blurring of vessel margin and no stair-step artifacts)
- Score 2 = fair  
(Visibly blurred vessel margin, clearly broader motion artifacts extending less than 5 mm from the vessel center, and stair-step artifacts  $<$  25% of the vascular diameter)
- Score 1 = poor

(Lack of vessel wall definition, presence of streak artifacts extending at least 5 mm from the center of the vessel and stair-step artifacts >25% of the vascular diameter)

### 3.7.6 Evaluate the quantitative image quality

Evaluate the quantitative image quality by determining image noise. Image noise is defined as the SD of CT No. in a ROI (100 mm<sup>2</sup>) placed in the aortic root at the level of the origin of the left main coronary artery.

### 3.7.7 Effective dose calculation

The effective dose is calculated from the equation:

$$\text{Effective dose} = \text{DLP} \times \text{conversion coefficient}$$

The conversion coefficient is 0.014 mSv/mGy.cm for chest[15].

## 3.8 Sample size

The sample population is independent, prospective data. So the sample size is determined by formula;

$$\begin{aligned} N &= (Z_{\alpha/2})^2 \sigma^2 / d^2 \\ &= (1.96)^2 (1.6)^2 / (0.49)^2 = 41 \text{ cases} \end{aligned}$$

By

$\alpha$	= 0.05
$Z_{\alpha/2}$	= 1.96
$d_{11}$	= Acceptable error (0.49)
$\sigma^2_{11}$	= Variance (1.6)
$\sigma^2, d$	Obtained from literature review [12].

## 3.9 Measurement

### Variables

Independent variables: acquisition protocol, scanning parameters

Dependent variables: CTDIvol, DLP, effective dose, image scoring and image noise



### 3.10 Statistical analysis

3.10.1 Descriptive statistics: mean, standard deviation (SD), minimum and maximum effective dose and image noise were determined with the excel program.

3.10.2 Weighted Kappa for interobserver reliability was used to evaluate qualitative image quality analysis from [www.medcalc.org/manual/kappa.php](http://www.medcalc.org/manual/kappa.php)

### 3.11 Data Collection

3.11.1 Patient information: age, gender, height, weight, body mass index (BMI), heart rate (bpm), HR variability, medication, contrast agent, acquisition protocol, kVp and mAs

3.11.2 The CTDIvol and DLP read out from CT monitor.

This data was collected at Computed Tomography Unit, Chulachakapong Building, 1<sup>st</sup> floor, Department of Radiology, King Chulalongkorn Memorial Hospital, Bangkok Thailand, using 320-detector row TOSHIBA Aquilion ONE.

### 3.12 Data Analysis

The verification of CTDIvol had been reported as percentage difference between the displayed and the measured for each kVp setting. After that the radiation dose data for specific parameter setting were collected from the values of CTDIvol and DLP displayed on the CT console in the unit of mGy and mGy.cm, respectively, presented in form of table and chart.

Data from patients had been reported as mean, standard deviation and ranges presented in form of table.

The data of CTDIvol and DLP displayed on CT console were obtained for the calculation of the effective dose for CCTA examination and presented in form of table and bar chart.

The qualitative image quality was analyzed by two radiologists using image scoring as presented in form of table. The quantitative image quality was analyzed by the image noise determining the standard deviation of mean HU in a ROI for each protocol. This data presented in form of bar chart.

### **3.13 Outcomes**

The patient effective dose was calculated by using the DLP from CCTA examination in each protocol. Qualitative image quality was scoring by two radiologists and quantitative image was determined by the image noise.

### **3.14 Expected Benefits**

The effective dose in CCTA and the image quality in each acquisition protocol are expected from this study. These would be beneficial to the patients and the radiologists in order to justify requesting the examination or further investigations. The patient dose reduction should be considered for the radiation safety for the patients.

### **3.15 Ethical consideration**

The radiation dose of CCTA is directly evaluated in patients. So, informed consent from every patient was obtained before the procedure. The Ethic Committee of Faculty of Medicine, Chulalongkorn University had approved this research proposal.

## CHAPTER IV

### RESULT

#### 4.1 Quality control of the CT scanner: TOSHIBA Aquilion ONE

The quality control of CT scanner was performed following AAPM report No.39 [13] and ImPACT Information Leaflet [14]. It includes the test of electromechanical component, image quality and radiation dose. In Table 4.1 and appendix B, the detail of quality control of CT scanner is shown with the summarized report of CT scanner performance test.

**Table 4.1** Report of CT system performance

Location	<u>CT unit, Chulachakapong Building, Floor.G</u>
Date	<u>February 12, 2011</u>
Manufacturer	<u>Toshiba</u>
Model	<u>Aquilion ONE</u>
<u>Pass</u>	Scan Localization Light Accuracy
<u>Pass</u>	Alignment of Table to Gantry
<u>Pass</u>	Table Increment Accuracy
<u>Pass</u>	Slice Increment Accuracy
<u>Pass</u>	Gantry Angle Tilt
<u>Pass</u>	Position Dependence and SNR of CT Numbers
<u>Pass</u>	Reproducibility of CT Numbers
<u>Pass</u>	mAs Linearity
<u>Pass</u>	Linearity of CT Numbers
<u>Pass</u>	Accuracy of Distance Measurement
<u>Pass</u>	Image uniformity
<u>Pass</u>	High Contrast Resolution
<u>Pass</u>	Low Contrast Detectability
<u>Pass</u>	Radiation Profile width

## 4.2 Verification of Computed Tomography Dose Index (CTDI)

### 4.2.1 CTDI<sub>100</sub> in air

Measure the CTDI<sub>100</sub> in air using head and body protocols and the 100 mm pencil chamber is set at the isocenter of the CT bore. The scan parameter is 100 mA tube current, 1 sec scan time and small focal spot size setting for all measurements at kilovoltage setting of 80, 100, 120 and 135. The results of CTDI in air are shown in Table 4.2.

**Table 4.2** The measured CTDI<sub>100</sub> in air for head and body protocols for each kVp.

kVp	CTDI <sub>100</sub> (mGy) in air in Head protocol							
	Slice Collimation in mm (NT)							
	1 (1x1)	2 (0.5x4)	4 (1x4)	8 (2x4)	12 (3x4)	16 (4x4)	20 (5x4)	32 (8x4)
<b>80</b>	6.36	7.72	10.1	15.09	19.92	24.85	29.69	43.93
<b>100</b>	10.49	12.79	16.83	24.85	32.91	40.97	48.98	72.33
<b>120</b>	15.97	19.31	25.25	36.97	48.55	60.27	72.12	106.12
<b>135</b>	21.34	25.51	32.88	47.58	62.25	76.87	91.45	134.29

**Table 4.2** The measured CTDI<sub>100</sub> in air for head and body protocols for each kVp.

kVp	CTDI <sub>100</sub> (mGy) in air in Body protocol							
	Slice Collimation in mm (NT)							
	1 (1x1)	2 (0.5x4)	4 (1x4)	8 (2x4)	12 (3x4)	16 (4x4)	20 (5x4)	32 (8x4)
<b>80</b>	6.70	7.73	9.67	13.52	17.15	20.98	24.86	NA
<b>100</b>	12.34	13.62	17.00	23.66	29.96	36.67	43.40	63.47
<b>120</b>	18.25	21.11	26.16	36.29	45.66	55.83	65.86	96.02
<b>135</b>	24.54	28.23	34.72	47.60	59.91	72.39	85.36	123.79

*\*As the 16 cm coverage exceeds the 10 cm dosimeter length, the correction factors for the kilovoltage peak value ranges 1.03-1.05 were applied [16].*

#### 4.2.2 CTDI<sub>100</sub> in head phantom

The CTDI<sub>100</sub> in head phantom was determined by using a 100 mm pencil ionization chamber placed in each hole of 16 cm diameter PMMA phantom at the isocenter of the CT bore. The scan parameters were 100 mA, 1 sec scan time, 180mm FOV and 2x4.0 mm collimation setting for all measurements at each kVp setting of 80, 100, 120 and 135. The result of CTDI in head phantom is shown in Table 4.3.

**Table 4.3** The measured CTDI<sub>100</sub> at each position of head phantom for each kVp.

kVp	CTDI <sub>100</sub> in head phantom (mGy)				
	At center	At peripheral			
		North	East	South	West
80	6.92	8.84	8.03	7.65	8.73
100	12.86	16.69	13.63	12.83	14.04
120	20.43	25.90	21.72	20.72	22.72
135	27.73	34.21	28.33	26.84	29.03

#### 4.2.3 CTDI<sub>100</sub> in body phantom

The CTDI<sub>100</sub> in body phantom was determined by using a 100 mm pencil ion chamber placed in each hole of 32 cm diameter PMMA phantom at the isocenter of the CT bore. The scan parameters were 100 mA, 1 sec scan time, 500 mm FOV and 2x4.0 mm collimation setting for all measurements at each kVp setting of 80, 100, 120 and 135. The result of CTDI in body phantom is shown in Table 4.4

**Table 4.4** The measured CTDI<sub>100</sub> at each position of body phantom for each kVp.

kVp	CTDI <sub>100</sub> in body phantom (mGy)				
	At center	At peripheral			
		North	East	South	West
80	1.75	4.28	4.54	3.84	4.27
100	3.83	8.45	9.22	7.70	9.27

**Table 4.4** The measured CTDI<sub>100</sub> at each position of body phantom for each kVp.

kVp	CTDI <sub>100</sub> in body phantom (mGy)				
	At center	At peripheral			
		North	East	South	West
120	6.83	13.54	13.59	12.47	13.17
135	9.73	18.82	18.23	16.61	21.49

#### 4.2.4 CTDI<sub>vol</sub> on monitor and calculated CTDI<sub>w</sub>

Determine the CTDI<sub>w</sub> by using the results in Table 4.3 and 4.4. The CTDI<sub>vol</sub> displayed on CT monitor were recorded to compare percentage difference with the calculated values as shown in Table 4.5 for CTDI<sub>vol</sub> in head phantom and Table 4.6 for CTDI<sub>vol</sub> in body phantom.

**Table 4.5** CTDI<sub>vol</sub> displayed on monitor and calculated CTDI<sub>w</sub> using head techniques mAs 100, collimation 8 mm and 180 mmFOV.

kVp	CTDI <sub>vol</sub> (mGy) in head phantom		
	Calculated	Displayed	% difference
80	7.78*	8.0	- 2.8
100	14.98*	14.6	2.6
120	23.32*	22.5	3.6
135	30.82*	29.7	3.7

\* As the 16 cm coverage exceeds the 10 cm dosimeter length, the correction factor ranges 1.08-1.1 for the kilovoltage peak value were applied [16].

CTDI<sub>vol</sub> displayed on the monitor and the calculated CTDI<sub>w</sub> using head techniques mAs 100, collimation 8 mm and 180 mmFOV are plotted in figure 4.1.

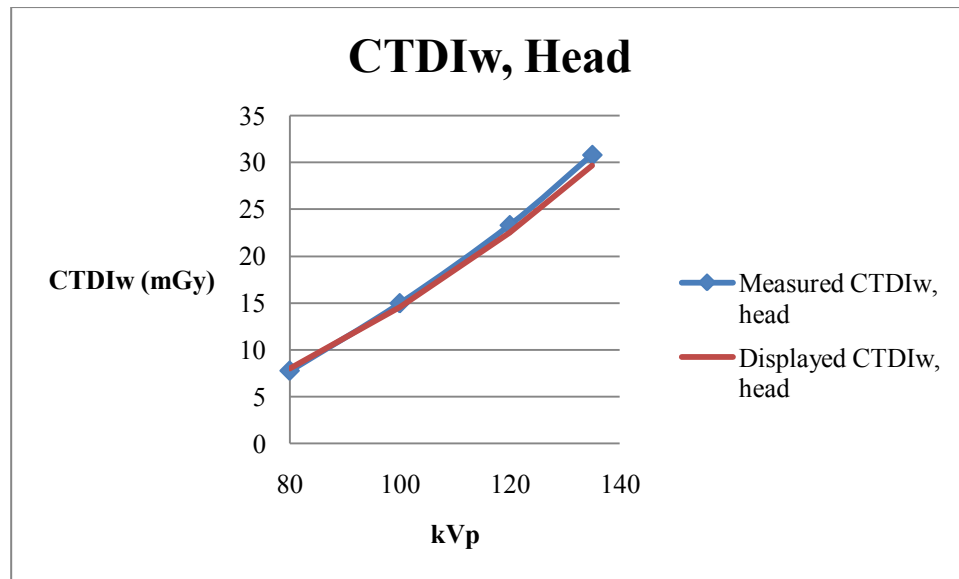


**Figure 4.1** CTDI<sub>vol</sub> (mGy) and CTDI<sub>w</sub> (mGy) of head phantom as the function of kVp are plotted in red and blue straight lines of less than 4 percent different.

**Table 4.6** CTDI<sub>vol</sub> displayed on monitor and calculated CTDI<sub>w</sub> using body techniques mAs 100, collimation 8 mm and 500 mmFOV.

kVp	CTDI <sub>vol</sub> (mGy) in body phantom		
	Calculated	Displayed	% difference
80	3.47*	3.5	- 0.9
100	7.33*	7.2	1.8
120	11.73*	11.8	0.6
135	16.38*	16.3	0.5

\* As the 16 cm coverage exceeds the 10 cm dosimeter length, the correction factor ranges 1.02-1.08 for the kilovoltage peak value were applied [16].

CTDI<sub>vol</sub> displayed on monitor and CTDI<sub>w</sub> using body techniques mAs 100, collimation 8 mm and 500 mmFOV are plotted as the function of kVp as in figure 4.2.

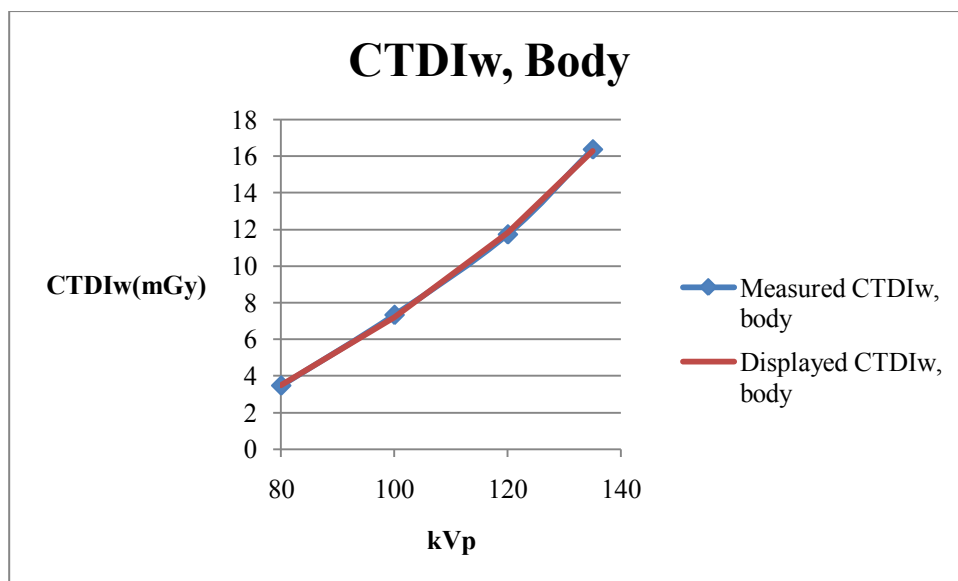


**Figure 4.2** CTDI<sub>vol</sub>(mGy) and CTDI<sub>w</sub>(mGy) of body phantom as the function of kVp are plotted in red and blue straight line of less than 2 percent different

### 4.3 Patient information and scanning parameters

41 patients completed consent form before coronary CTA examination. Patients whose heart rates were more than 65 bpm were given Metoprolol 50-100 mg 1 hour prior to the scanning to slow down and stabilize it. The patient data and scanning parameters were shown in Table 4.7

**Table 4.7** Patient information and scanning parameters

Case No.	Age (Yrs)	Gender (M, F)	BMI (kg/m <sup>2</sup> )	kVp	mA	HR (bpm)	Protocol
1	56	F	31	120	500	52	Prospective70-80% 1RR
2	74	F	22	120	350	63	Prospective70-80% 1RR
3	45	M	27	120	400	54	Prospective70-80% 1RR
4	65	F	23	120	350	52	Prospective70-80% 1RR
5	73	F	27	120	400	64	Prospective70-80% 1RR
6	48	M	25	120	350	60	Prospective70-80% 1RR
7	75	M	23	120	350	50	Prospective70-80% 1RR
8	74	M	31	120	500	65	Prospective70-80% 1RR
9	52	M	31	120	500	64	Prospective70-80% 1RR



**Table 4.7** Patient information and scanning parameters

Case No.	Age (Yrs)	Gender (M, F)	BMI (kg/m <sup>2</sup> )	kVp	mA	HR (bpm)	Protocol
10	73	M	21	120	350	63	Prospective70-80% 1RR
11	77	F	28	120	400	65	Prospective70-80% 1RR
12	76	F	30	120	400	65	Prospective70-80% 1RR
13	33	F	25	120	350	65	Prospective70-80% 1RR
14	52	M	20	120	300	60	Prospective70-80% 1RR
15	74	M	20	120	300	60	Prospective70-80% 1RR
16	60	M	26	120	400	60	Prospective70-80% 1RR
17	54	F	21	120	350	56	Prospective70-80% 1RR
18	51	F	25	120	350	65	Prospective70-80% 1RR
19	58	M	25	120	350	65	Prospective70-80% 1RR
20	64	F	24	120	350	58	Prospective70-80% 1RR
21	69	F	31	120	500	57	Prospective70-80% 1RR
22	62	F	25	120	350	50	Prospective70-80% 1RR
23	39	M	29	120	400	60	Prospective70-80% 1RR
24	52	F	25	120	350	51	Prospective70-80% 1RR
25	51	F	23	120	350	64	Prospective70-80% 1RR
26	53	M	22	120	350	58	Prospective70-80% 1RR
27	63	F	25	120	350	65	Prospective70-80% 1RR
28	69	M	23	120	350	65	Prospective70-80% 1RR
29	66	F	30	120	400	41	Prospective70-80% 1RR
30	60	M	29	120	400	62	Prospective70-80% 1RR
31	56	M	26	120	400	70	Prospective30-80% 1RR
32	77	M	20	120	300	70	Prospective30-80% 1RR
33	52	M	19	120	300	69	Prospective30-80% 1RR

**Table 4.7** Patient information and scanning parameters

Case No.	Age (Yrs)	Gender (M, F)	BMI (kg/m <sup>2</sup> )	kVp	mA	HR (bpm)	Protocol
34	36	F	25	120	350	74	Prospective30-80% 2RR
35	57	F	21	120	350	73	Prospective30-80% 2RR
36	64	F	28	120	400	71	Prospective30-80% 2RR
37	80	M	21	120	350	75	Retrospective*
38	72	M	20	120	300	72	Retrospective*
39	50	F	21	120	350	65	Retrospective*
40	58	M	23	120	350	80	Retrospective*
41	49	M	25	120	350	75	Retrospective*

\* *Retrospective with tube current modulation*

#### 4.4 Radiation dose

CTDI<sub>vol</sub> and DLP were recorded from monitor. To calculate the effective dose, DLP was multiplied by conversion coefficient of 0.014 mSv/mGy.cm for chest [15].

**Table 4.8** Average CTDI<sub>vol</sub>, DLP and Effective dose from coronary CTA of 41 patients in 4 protocols of various heart rates.

Protocol	N	CTDI <sub>vol</sub> (mGy)	DLP(mGy.cm)	Effective dose(mSv)
1. PGT 70-80% 1RR	30	14.5	260.5	3.6 ± 0.9
2. PGT 30-80% 1RR	3	31.1	448.2	6.3 ± 1.9
3. PGT 30-80% 2RR	3	46.7	767.0	10.8 ± 1.8
4. RGT with tube current modulation	5	49.3	868.0	12.1 ± 7.7

Effective dose from coronary CTA is plotted against 41 patients of 4 protocols as in figure 4.3

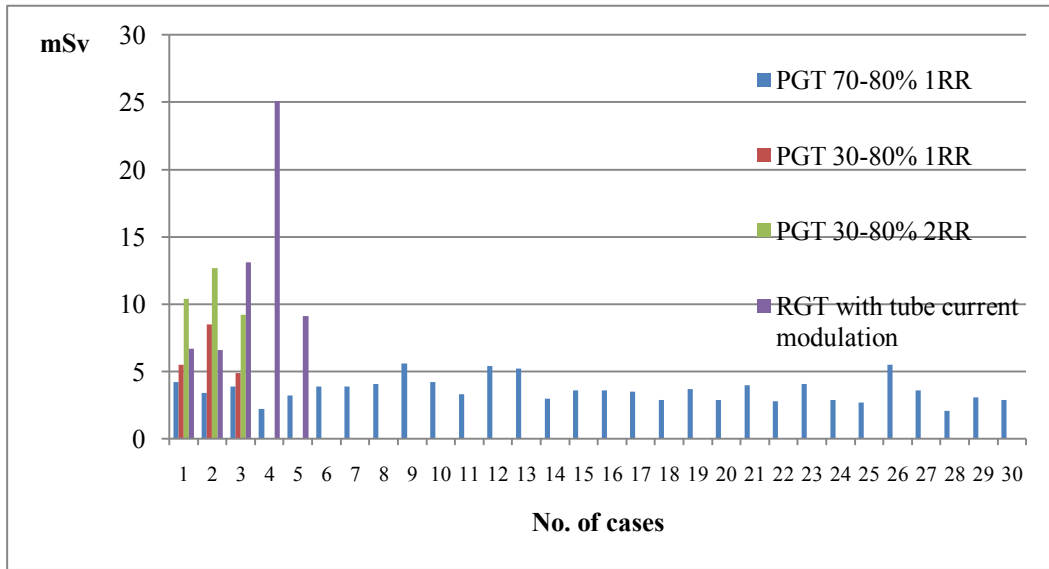


Figure 4.3 Bar chart of the effective dose from 41 patients underwent coronary CTA

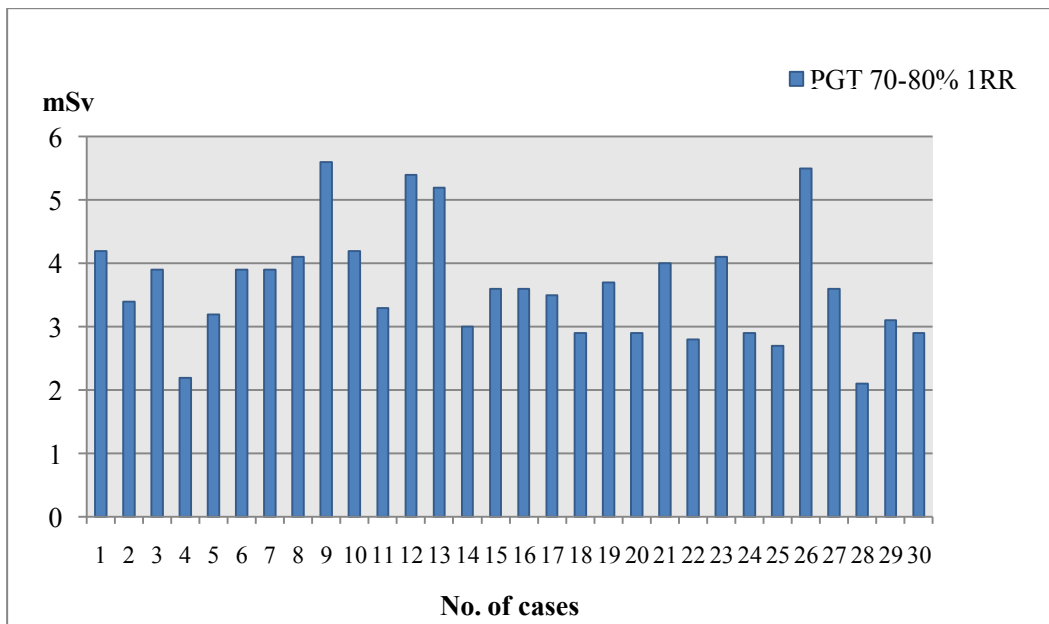
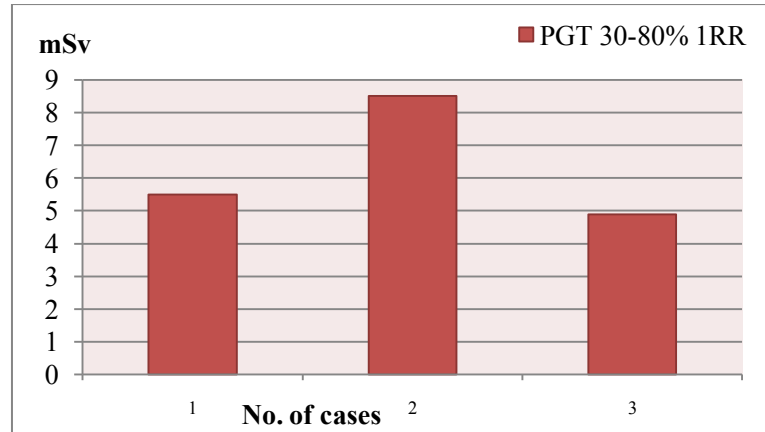
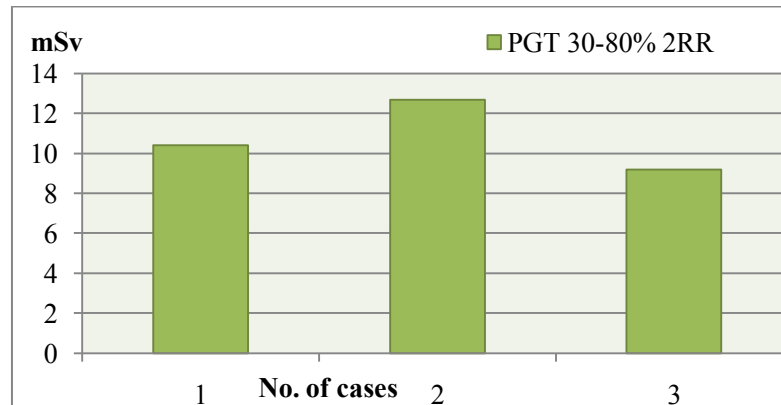


Figure 4.4 Bar chart of the effective dose from 30 patients in PGT 70-80% 1RR



**Figure 4.5** Bar chart of the effective dose from 3 patients in PGT 30-80% 1RR



**Figure 4.6** Bar chart of the effective dose from 3 patients in PGT 30-80% 2RR

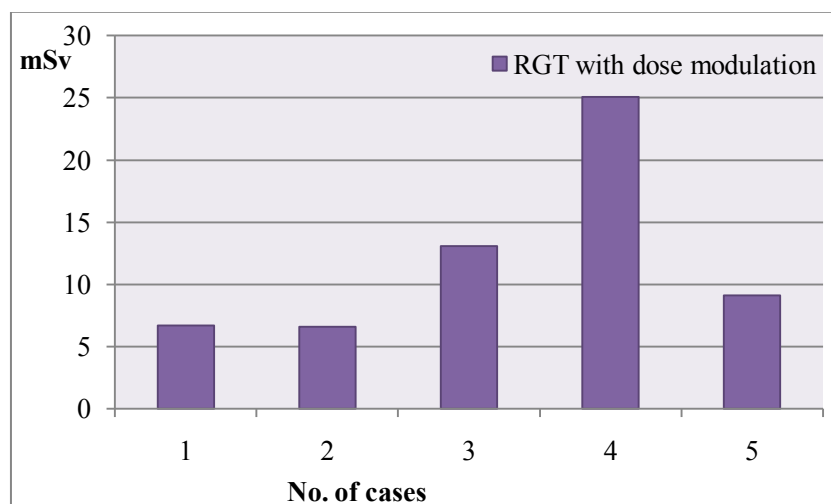


**Figure 4.7** Bar chart of the effective dose from 5 patients in RGT with dose modulation

Bar chart 4.8 Compare the effective dose with other studies

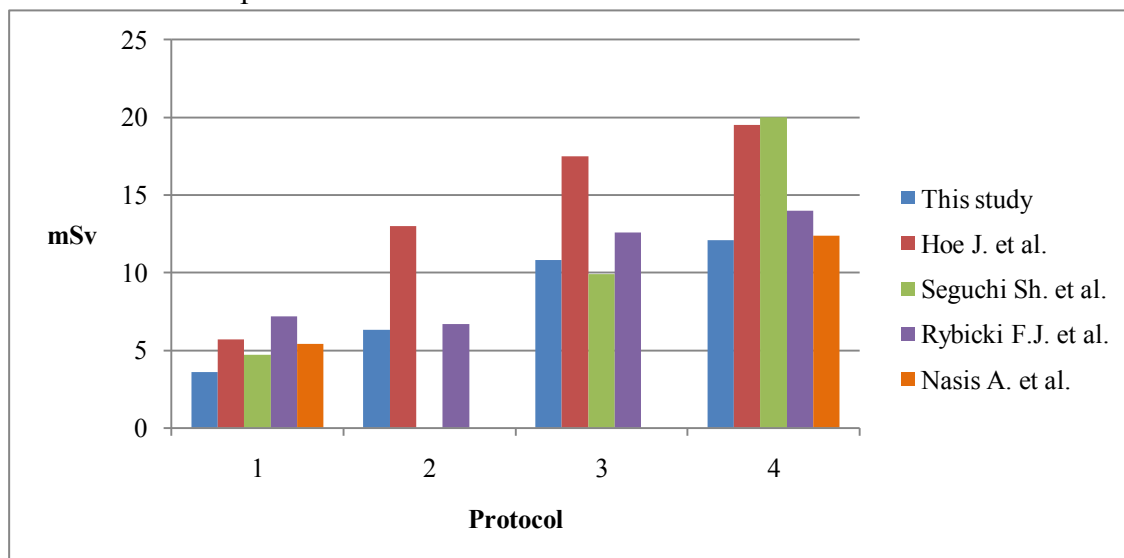


**Figure 4.8** Effective dose, mSv from 41 patients, underwent coronary CTA in 4 protocols was compared to other studies.

All of studies were scanned from 320-detector rows CT, Toshiba Aquilion ONE. The details of protocol are shown in Table 4.9

**Table 4.9** Patient protocol compared with other studies

Protocol	1	2	3	4
This study	PGT 70-80% 1RR	PGT 30-80% 1RR	PGT 30-80% 2RR	RGT*
Hoe J.[12]	PGT 65-100% 1RR	PGT 30-90% 2RR	PGT 30-90% 3RR	RGT* 3-5RR
Seguchi Sh.[16]	PGT 62-78% 1RR	-	PGT 70% 2RR	RGT*
Rybicki F J.[11]	PGT 70-85% 1RR	PGT 60-100% 1RR	PGT 60-100% 2RR	RGT
Nasis A. [6]	PGT 60-100%	-	-	RGT*

\* *Retrospective gating with tube current modulation*

For 30 patients in PGT 70-80%, when separate the effective dose from the BMI of the patient are shown in Figure 4.9

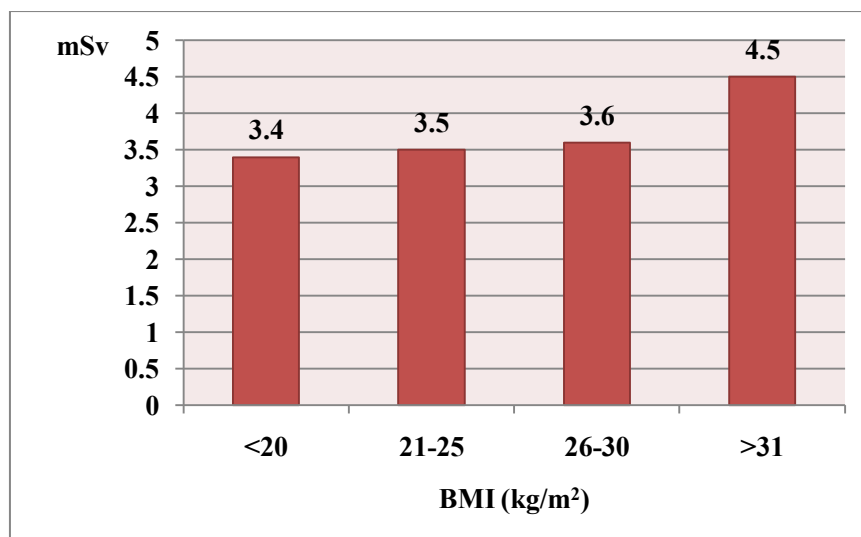


**Figure 4.9** Effective dose, mSv from 30 patients from PGT 70-80% 1RR in 4 range of BMI.

## 4.5 Image quality

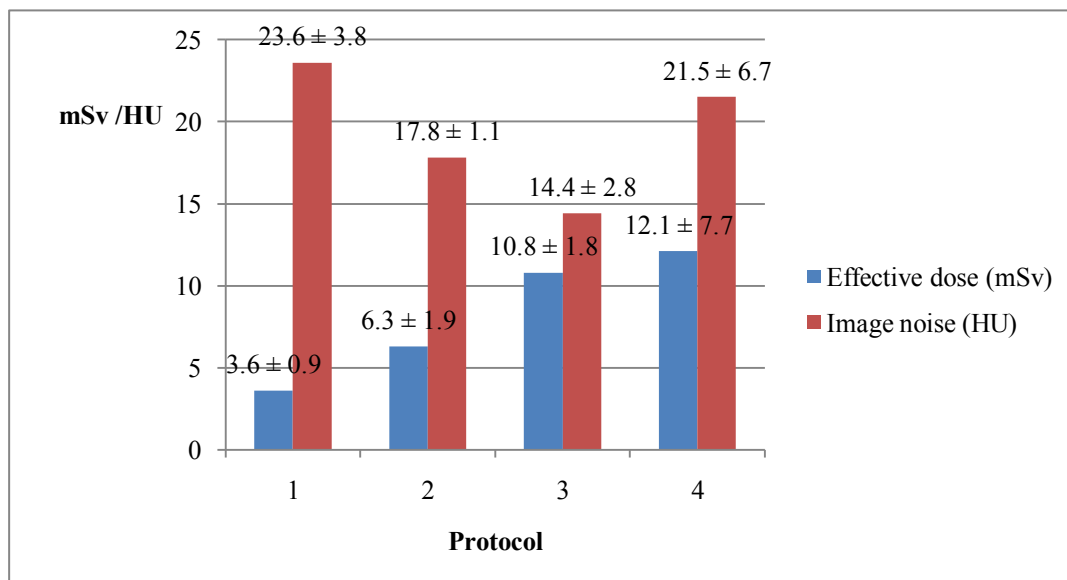
### 4.5.1 Quantitative image quality

Image noise was defined as the standard deviation (SD) of CT Number, in a ROI (100 mm<sup>2</sup>) at the aortic root at the level of the origin of the left main coronary artery. The noise data is calculated and displayed in table 4.10

**Table 4.10** Image noise

Protocol	N	Image noise (HU)
1. PGT 70-80% 1RR	30	23.6 ± 3.8
2. PGT 30-80% 1RR	3	17.8 ± 1.1
3. PGT 30-80% 2RR	3	14.4 ± 2.8
4. RGT with dose modulation	5	21.5 ± 6.7

Bar chart 4.3 Image noise and the effective dose are plotted as bar chart as in figure 4.5 for 4 protocols.



**Figure 4.10** Bar chart of image noise and the effective dose

#### 4.5.2 Qualitative image quality

Qualitative image qualities were evaluated by two radiologists from criteria score 4 to 1 as described in the chapter III. Table 4.11 and 4.12 are shown the scored from 1 radiologist with high experience.

**Table 4.11** Overall Image scoring

Score	RCA	LMA	LAD	LCX
4 = Excellent	18(43.9%)	25(60.1%)	18(43.9%)	17(41.5%)
3 = Good	16(39.0%)	16(39.0%)	21(51.2%)	18(43.9%)
2 = Fair	7(17.1%)	0(0%)	2(4.9%)	6(14.6%)
1 = Poor	0(0%)	0(0%)	0(0%)	0(0%)
Total	41	41	41	41

\* *Weighted Kappa* = 0.652 ([www.medcalc.org/manual/kappa.php](http://www.medcalc.org/manual/kappa.php))

**Table 4.12** Image scoring in each protocol

Protocol	Vessel	4 = Excellent	3 = Good	2 = Fair	1 = Poor	Total
1	RCA	11	14	5	0	30
	LMA	18	12	0	0	30
	LAD	10	19	1	0	30
	LCX	10	16	4	0	30
		39(40.8%)	61(50.8%)	10(8.3%)	0(0%)	120(100%)
2	RCA	1	1	1	0	3
	LMA	1	2	0	0	3
	LAD	1	1	1	0	3
	LCX	1	1	1	0	3
		4(33.3%)	5(41.7%)	3(25.0%)	0(0%)	12(100%)
3	RCA	2	1	0	0	3
	LMA	2	1	0	0	3
	LAD	2	1	0	0	3
	LCX	2	1	0	0	3
		8(66.7%)	4(33.3%)	0(0%)	0(0%)	12(100%)
4	RCA	4	0	1	0	5
	LMA	4	1	0	0	5
	LAD	5	0	0	0	5
	LCX	4	0	1	0	5
		17(85%)	1(5%)	2(10%)	0(0%)	20(100%)



## CHAPTER V

### DISCUSSION AND CONCLUSION

#### 5.1 Discussion

Quality control of CT system is very important and should be firstly performed. All the measured CT Dose was evaluated following the AAPM No.39 protocol using the conventional ionization chamber of 100 mm length. As new CT scanner is equipped with a 320 detector row which allows a longitudinal coverage of 160 mm in one rotation. So 100 mm pencil chamber is no more appropriate for measuring the computed tomography dose index in air (CTDI in air) and weighted computed tomography dose index (CTDI<sub>w</sub>) value. Geleijns J, et al [17] studied CT dose assessment for a 160 mm wide, 320 detector row by comparing the standard measurements with 300 mm chamber. Correction factor (1.02 -1.1) for standard dosimetry equipment was applied to 320-detector row CT measurement to estimate dose with the use of conventional method.

CTDI<sub>100</sub> in air was measured in head and body protocols in all slice collimation and all kVp. The CTDI<sub>100</sub> in air values increased from small to large slice collimation and increase from 80 kVp to 135 kVp in head protocol. Similar results were recorded for the CTDI<sub>100</sub> in air values in body protocol.

The calculated CTDI<sub>vol</sub> was higher than the displayed CTDI<sub>vol</sub> values in all kVp setting for head protocol except at 80 kVp. The percentage differences of calculated CTDI<sub>vol</sub> values were less than 4 ranging from -2.8 to 3.7. For body protocol, the calculated CTDI<sub>vol</sub> was higher than the displayed CTDI<sub>vol</sub> values in all kVp setting except in 80 kVp too. The percentage differences of calculated CTDI<sub>vol</sub> values were less than 2 ranging from -0.9 – 1.8.

From the IAEA Technical Report Series (TRS) No.457: Dosimetry in Diagnostic Radiology: An International Code of Practice [18], the discrepancy between the measurement and the displayed values came from the measurement uncertainty. The factors affect the measurement uncertainty to estimate the CTDI were the characteristics of ionization chamber and electrometer, the measurement scenario, the precision of reading, tube loading, chamber positioning, the phantom construction, the chamber response in phantoms and the inaccuracy on laser beam alignment.

Forty one consecutive patients were scanned using protocol 1-4 according to the heart rates. The patient's heart rate were controlled to keep low heart rate so 30 patients used protocol PGT 70-80% 1R-R interval acquisition, 3 patients used protocol 2 (PGT 30-80% 1R-R interval acquisition), 3 patients used protocol 3 (PGT 30-80% 2R-R) and 5 patients used protocol 4 (RGT with tube current modulation). The patient information consisted of 21 male and 20 female, mean ages were 60.6, 61.7, 52.3 and 61.8 years and mean BMI were 25.6, 21.8, 24.6 and 21.6 kg/m<sup>2</sup> in

protocol 1 to 4, respectively. Some of the patients heart rate was less than 65 bpm but RGT was used because of the heart rate variability.

CTDI<sub>vol</sub> in PGT was lowest of 14.5 mGy in PGT 70-80% 1R-R and the highest is 49.3 mGy in RGT with tube current modulation. In PGT, the CTDI<sub>vol</sub> is increasing in 14.5, 31.1 to 46.7 mGy in phase window 70-80% 1R-R, 30-80% 1R-R and 30-80% 2R-R, respectively. Effective radiation dose was estimated from the DLP and a conversion factor of 0.014 mSv/mGy.cm [15]. The lowest effective dose was  $3.6 \pm 0.9$  mSv in PGT 70-80% 1R-R and increased in PGT 30-80% 1R-R =  $6.3 \pm 1.9$  mSv, PGT 30-80% 2 R-R =  $10.8 \pm 1.8$  mSv and the highest was  $12.1 \pm 7.7$  mSv in RGT with tube current modulation. The highest dose in case no. 4 of the RGT with tube current modulation was 25.1 mSv because of using 3 R-R.

In comparison to other studies [12], [16], [11], [6] with similar acquisition protocols, the effective dose in our study is lowest among the others because of the narrow window width. Steigner ML, et al [19] studied the narrowing phase window width in prospectively ECG-gated single heart beat in 320-detector row coronary CT angiography, and concluded that the phase window width of 10% reduced patient radiation and yield diagnostic images in more than 90% of patients but heart rate control is still an important component of 320-detector row prospectively gated CT dose reduction. In PGT 1 R-R, our study phase window width at 10% from 70-80% so the radiation dose is lower than Hoe J [12] 65-100% 1R-R, Segushi SH [16] 62-78%, Rybicki FJ [11] 70-85% and Nasis A [6] 60-100% 1R-R. The radiation dose increased if scanned more than one heart beat. For retrospective ECG gated, the radiation dose was higher than prospective ECG gated because of more exposure in R-R interval. One method to reduce radiation dose is the use of tube current modulation [20]. Although the radiation dose in retrospective with tube current modulation was higher than prospective gated but this technique can reduce the patient dose from retrospective technique with full exposure. This technique can be a choice in the patient with uncontrollable high heart rate or non stable heart rate.

Besides the acquisition mode, the mA and kVp settings also affect the patient dose. In our study, the mA and kVp setting depend on BMI of the patient.

In the part of quantitative image quality, image noise in PGT 70-80% 1R-R was  $23.6 \pm 3.8$  HU which was the highest and decreasing in PGT 30-80% 1R-R to  $17.8 \pm 1.1$  HU, in PGT 30-80% 2R-R to  $14.4 \pm 2.8$  HU. The image noise in RGT with tube current modulation was  $21.5 \pm 6.7$  HU.

For overall qualitative image scored by two radiologists (weighted kappa value = 0.652) shown good agreement, in RCA the score was excellent 43.9%, good 39.0%, fair 17.0% and poor 0% score. The score of LMA was excellent 60.1%, good 39.0%, fair and poor 0% score. The score of LAD was excellent 43.9%, good 51.2%, fair 4.9% and poor 0% score. The score of LCX was excellent 41.5%, good 43.9%, fair 14.6% and poor 0% score.

In each protocol, the score in PGT 70-80% 1R-R was excellent 40.8%, good 50.8% and fair 8.3%. In the PGT 30-80% 1R-R the score was excellent 33.3%, good 41.7% and fair 25%. In PGT 30-80% 2R-R was excellent 66.7% and good 33.3%. In RGT with tube current modulation were excellent 86%, good 5% and fair 10%.

The limitations in this study are, first, the direct measurement of patient dose using the gold standard method of TLD has not performed, the segmental vessel image qualities not analyze and the numbers of cases are not uniform for each protocol.

## 5.2 Conclusion

Our CTDI measurements provide the CTDI data to verify radiation dose with the display monitor at work station. The calculated CTDI and DLP value and the monitor value were different at less than  $\pm 5\%$  percent. Therefore, the CTDI and DLP values on monitor can be confidently used to evaluate the patient dose. The effective dose was obtained by DLP multiply by the conversion coefficients at the region specific coefficients. The data could be obtained from European Commissioning.

Coronary Angiography studied by 320-detector row computed tomography at King Chulalongkorn Memorial Hospital, the  $CTDI_{vol}$  in PGT 70-80% 1R-R was lowest at 14.5 mGy and the highest was obtained in RGT with tube current modulation 1-3 R-R at 49.3 mGy. The effective dose in PGT 70-80% 1R-R was lowest at  $3.6 \pm 0.9$  mSv, in PGT 30-80% 1R-R and 2R-R and were  $6.3 \pm 1.9$  and  $10.8 \pm 1.8$  mSv, respectively. In RGT with tube current modulation, the effective dose was highest at  $12.1 \pm 7.7$  mSv.

Image noise was the highest in PGT 70-80% 1R-R and decreased in RGT with tube current modulation, PGT 30-80% 1R-R and lowest in PGT 30-80% 2 R-R. Overall qualitative image quality was mostly good to excellent score.

In CCTA, the heart rate, the heart rate variability and the diseasing of the patient affect the radiation dose and image quality so the suitable acquisition protocol must be optimized. Besides that, the considerations of patient weight and height, also affect the radiation dose and image quality.

In conclusion, our study shows that in patients with low heart rate, PGT 70-80% 1 R-R in 320-detector row CT lower radiation dose and good to excellent image quality could be obtained because of the narrowing phase window width and single heart beat. In higher heart rate patient, more phase window and more heart beat could be used. In addition, the RGT with tube current modulation, the effective dose was higher than PGT but lower than RGT with full dose exposure [20] so can be used in higher heart rate for good diagnostic.

### **5.3 Recommendation**

Prospective gating technique with narrowing the exposure window and single heartbeat was recommended for performing 320-detector row CCTA to get the acceptable image quality in the lowest effective dose for the patient. Pre-examination HR controlling less than 65% R-R interval is still necessary for the highest dose reduction. The optimization between dose and image quality must be concerned for the radiation safety to patients.

## REFERENCES

- [1] The ImPACT Group. Multi-slice CT scanners CEP08007. Medical Physics Bence Jones Offices Perimeter Road Tooting London UK : impactscan.org, 2009.
- [2] Thomas AG. Cardiovascular Disease in the Developing World and Its Cost-Effective Management. Circulation 112 (Sep 2005) : 3547-3553.
- [3] Mahadevappa M and Dianna D. Physics Tutorial for Residents Physics of Cardiac Imaging with Multiple-Row Detector CT. RadioGraphics 27 (Sep 2007) : 1495-1509.
- [4] Shrimpton PC, Hillier MC, Lewis MA and Dunn M. Doses from Computed Tomography (CT) Examinations in the UK - 2003 Review. Health Protection Agency, Chilton, Didcot, Oxon: NRPB-W67, 2008.
- [5] Mahesh M. Cardiac imaging : Technical Advances in MDCT compared with Conventional X-ray Angiography. US cardiology (2006) : 115-119.
- [6] Nasis A, Leung MC, Antonis PR, Cameron JD, Lehman SJ, Hope SA, Crossett MP, Troupis JM, Meredith IT and Sujith K. Diagnostic Accuracy of Noninvasive Coronary Angiography with 320-Detector Row Computed Tomography. The American Journal of Cardiology 106 (June 2010) : 1429-1435.
- [7] Hausleiter J, Meyer T, Hadamitzky M, Huber E, Zankl M, Martinoff S, Kastrati A and Schomig A. Radiation dose estimation from multislice CT in daily practise : Impact of different scanning protocols on effective dose estimates. Circulation 113 (Mar 2006) : 1305-1310.
- [8] Yang LH, Wu DK, Chen CY, Liu GC, Hsieh TJ, Jaw TH, Huang SY, Lin CC and Hsu JS. Quantitative Assessment of Image Quality 64-Slice CT of Coronary Arteries in Subjects Undergoing Screening for CAD. Kaohsiung J Med Sci 26 (2010) : 9-21.
- [9] Chen LK, Wu TH, Yang CC, Tsai CJ, Lee JSS. Radiation dose to patients and image quality evaluation from coronary 256-slice CTA. Nuclear Instruments and Methods in Physics Research A619 (Nov 2009) : 368-371.
- [10] Duate R, Fernandez G, Castellon D and Joao C Costa. Prospective Coronary CT Angiography 128 MDCT Versus Retrospective 64 MDCT: Improved Image Quality and Reduced Radiation Dose. HLC 906 (May 2010): 1-7.

- [11] Rybicki FJ , Otero HJ, Steigner ML, Vorobiof G, Nallamshetty L, Mitsouras D, Ersoy H, Coyner K and Di Carli MF. Initial evaluation of coronary images from 320-detector row computed tomography. Int J Cardiovasc Imaging. 24 (Mar 2008): 535-546.
- [12] Hoe J and Toh KH. First experience with 320-row multidetector CT coronary angiography scanning with prospective ECG to reduce radiation dose. Journals of Cardiovascular Computed Tomography. 3(May 2009) : 257-261.
- [13] American Association of Physicist in Medicine. Specification and acceptance testing of computed tomography scanners, report 39 (May 1993).
- [14] ImPACT. ImPACT information leaflet 1: CT scanner acceptance testing. Version 1.02 (2001) : 1-8.
- [15] European Working Group for Guidelines on quality criteria in CT (2004).
- [16] Seguchi SH, Aoyama T, Koyama SH, Fujii K and Yamauchi CH. Patient radiation dose in prospectively gated axial CT coronary angiography and retrospectively gated helical technique with a 320-detector row CT scanner. American Association of Physicists in Medicine. 37 (Nov 2010) : 5579-5585.
- [17] Geleijns J, Salvado Artells M, de Bruin PW, Matter R, Muramatsu Y and McNitti-Gray MF. Computed tomography dose assessment for a 160 mm wide, 320 detector row, cone beam CT scanner. Phys Med Bio. 54 (May 2009): 3141-3159.
- [18] International Atomic Energy Agency 2007. Dosimetry in Diagnostic Radiology: An International Code of Practice – Vienna : International Atomic Agency . Technical report series, ISSN 0074-1914 ; no.457.
- [19] Steigner ML, Otero HJ, Cai T, Mitsouras D, Nallmshetty L, Whitmore AG, Ersoy H, Levit NA, Di Carli MF and Rybicki FJ. Narrowing the phase window width in prospectively ECG-gated single heart beat 320-detector row coronary CT angiography. Int J Cardiovasc Imaging. 25 (July 2008) : 85-90.
- [20] Hausleiter J, Meyer T, Hadamitzky M, Huber E, Zankl M, Martinoff S, Kastrati A and Schomig A. Radiation Dose estimates from cardiac multislice computed

tomography in daily practice: Impact of different scanning protocols on effective dose estimates. American Heart Association.113 (Mar 2006) : 1305-1310.

## **Appendices**



## Appendix A: Case Record Form

**Table 1** Data Collection form of patient information

### Part 1: Radiation dose

<b>Clinical data collection sheet for radiation dose in coronary angiography</b>	
<b>Computed tomography at diagnostic radiology unit</b>	
<b>D/M/Y</b>	
<b>Patient study number</b>	
<b>Height (cm)</b>	
<b>Weight (kg)</b>	
<b>gender</b>	
<b>Age</b>	
<b>BMI</b>	
<b>HR(bpm)</b>	
<b>HR variability</b>	
<b>Protocol</b>	
<b>kV</b>	
<b>mAs</b>	
<b>Slice Collimation Thickness (mm)</b>	
<b>CTDI vol (mGy)</b>	
<b>DLP (mGy.cm)</b>	
<b>Effective Dose (mSv)</b>	

**Part 2: Image quality scores (1-4)**

**Table 2** Data Collection form of image score

<b>Clinical data collection sheet for image quality scoring (1-4)</b>				
Case No.	Right Coronary Artery (RCA)	Left Main Coronary Artery (LMA)	Left Anterior Descending Artery (LAD)	Left Circumflex Artery (LCX)
01				

:

<b>Clinical data collection sheet for image quality scoring (1-4)</b>				
Case No.	Right Coronary Artery (RCA)	Left Main Coronary Artery (LMA)	Left Anterior Descending Artery (LAD)	Left Circumflex Artery (LCX)
41				

## Appendix B: Quality Control of CT system

### 1. Scan Localization Light Accuracy

- Purpose:** To test congruency of scan localization light and scan plane.
- Method:** Tape Localization film to the backing plate making sure that the edges of the film are parallel to the plate edge. Place the film vertically along the midline of the couch aligned with its longitudinal axis. Raise the table to the head position. Turn the alignment light. Mark both internal and external light with unique pin pricks along the midline of the light. Expose the internal light localization using the narrowest slice setting at 120-140 kVp, 50-100 mAs. For external light increment table to light position under software control and expose the film.
- Tolerance:** The center of the irradiation field from the pin pricks should be less than 2 mm.

**Results:**

---

Measured Deviation	External	0	mm
	Internal	1.5	mm

---

**Comments:** Pass

### 2. Alignment of Table to Gantry

- Purpose:** To ensure that long axis of the table is horizontally aligned with a vertical line passing through the rotational axis of the scanner.
- Method:** Locate the table midline using a ruler and mark it on a tape affixed to the table. With the gantry untilted, extend the table top into gantry to tape position. Measure the horizontal deviation between the gantry aperture centre and the table midline.
- Tolerance:** The deviation should be within 5 mm.

**Results:**

---

	Table	Bore
Distance from Right to Center (mm)	236	359
Distance from Centre to Left (mm)	234	361

<b>Measured Deviation (mm)*</b>	<b>1</b>	<b>1</b>
---------------------------------	----------	----------

---

*\*Measured deviation = (Distance from right to center – Distance from center to left)/2*

**Comments:** Pass

### 3. Table Increment Accuracy

**Purpose:** To determine accuracy and reproducibility of table longitudinal motion.

**Method:** Tape a measuring tape at the foot end of the table. Place a paper clip at the center of the tape to function as an indicator. Load the table uniformly with 150 lbs. From the initial position move the table 300, 400 and 500 mm into the gantry under software control. Record the relative displacement of the pointer on the ruler. Reverse the direction of motion and repeat. Repeat the measurements four times.

**Tolerance:** Positional errors should be less than 3 mm at 300 mm position.

#### Results:

---

Indicated (mm)	Measured (mm)	Deviation (mm)
500	500	0
400	400	0
300	299	1
- 300	- 300	0
- 400	- 400	0
- 500	- 500	0

---

*\*Deviation = | Indicated – Measured|*

**Comments:** Pass

### 4. Slice Increment Accuracy

**Purpose:** To Determine the accuracy of the slice increment.

**Method:** Set up as you would for beam profile measurement. Select 120 kVp, 100 mAs, and smallest slit width. Perform several scans with different programmed slice separations under auto control. Scan the film with a densitometer and measure the distance between the peaks.

**Tolerance:** Position errors should be less than 3 mm at 300 mm position.

**Results:**


---

Slice Separation in mm	Measured Separation in mm	Deviation (mm)
20	20	0
30	30	0
50	50	0

---

$$*Deviation = |Slice\ separation - Measured\ separation|$$

**Comments:** Pass

**5. Gantry Angle Tilt**

**Purpose:** To determine the limit of gantry tilt and the accuracy of tilt angle indicator.

**Method:** Tape a localization film to the backing plate making sure that the edges of the film are parallel to the edges of the backing plate. Place the film vertically along the midline of the couch aligned with its longitudinal axis. Raise the table to the head position. Move the table into the gantry. Center plate to alignment light. Expose the film at inner light location using narrowest slit, 120-140 kVp, 50-100 mAs. Tilt the gantry to one extreme from the console. Record the indicated gantry angle. Expose the film using the above technique. Measure the clearance from the closest point of gantry to midline of the table.

Tilt the gantry to its extreme in the opposite direction. Record clearance and repeat the exposure. Measure the tilt angles from the images on the film.

**Tolerance:** Deviation between indicated and measured tilt angles  $\leq 30$ . Gantry clearance should be  $\geq 30$  cm.

**Results:**


---

	Away	Toward
Indicated Angle	15°	15°
Measured Angle	15°	15°
Deviation*	0	0

---

$$*Deviation = |Indicated\ angle - Measured\ angle|$$

**Comments:** Pass

## 6. Position Dependence of CT Numbers

**Method:** Position the water phantom centered in the gantry. Using 1 cm slice thickness, obtain one scan using typical head technique. Select a circular region of interest of approximately 400 sq. mm. and then record the mean C.T. number and standard deviation for each of the positions 1 through 5.

**Technique:** 120 kVp, 250 mA, 1 sec, slice collimation 8 mm. 180 mmSFOV.

**Tolerance:** The coefficient of variation of mean CT numbers of the four scans should be less than 0.2.

### Results:

Position	Mean C.T. #	S.D.	C.V.
1	113.3	11.0	0.097
2	113.3	12.0	0.106
3	115.8	11.6	0.100
4	113.4	12.9	0.114
5	113.7	9.8	0.086

\* $CV = \text{Standard deviation}/\text{mean CT number}$

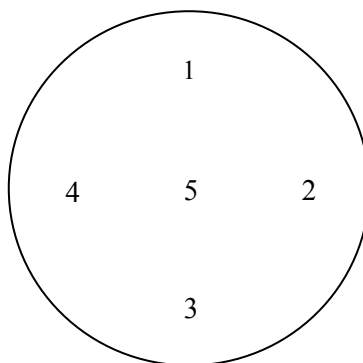


**Figure I** Position of ROI for CT number measurement.

**Comments:** Pass

## 7. Reproducibility of CT Numbers.

**Method:** Using the same set up and technique as position dependence, obtain three scans. Using the same ROI as position dependence in location 5,

this is the center of the phantom obtain mean C.T. numbers for each of the four scans.

**Tolerance:** The coefficient of variation of mean CT numbers of the four scans should be less than 0.002.

**Results:**

Run Number	1	2	3	4
Mean CT Number (HU)	113.21	113.27	113.42	113.46

<b>Mean Global C.T. Number</b>	113.34
<b>Standard Deviation</b>	0.119
<b>Coefficient Of variation</b>	0.001

**Comments:** Pass

### 8. mAs Linearity

**Method:** Set up the same as position dependence and insert 10 cm long pencil chamber in the center slot of the C.T. dose head phantom. Select the same kVp and time as used for head scan. Obtain four scans in each of the mA stations normally used in the clinic. For each mA station record the exposure in mGy for each scan. Scans should be performed in the increasing order of mA. Compute mGy/mAs for each mA setting.

**Technique:** 120 kVp, 250 mA, 1 sec, 180 mmSFOV

**Results:**

mA	Exposure in mGy				mGy/mAs	C.V.
	Run 1	Run 2	Run 3	Run 4		
50	1.018	1.011	1.017	1.02	0.02	1.000
100	2.037	2.041	2.022	2.02	0.02	0.001
200	4.064	4.055	4.017	4.024	0.02	0.002
250	5.025	5.017	5.034	5.023	0.02	0.003

300	6.923	6.869	6.868	6.932	0.02	0.067
400	9.228	9.225	9.242	9.172	0.02	0.001
500	11.54	11.44	11.42	11.42	0.02	0.003

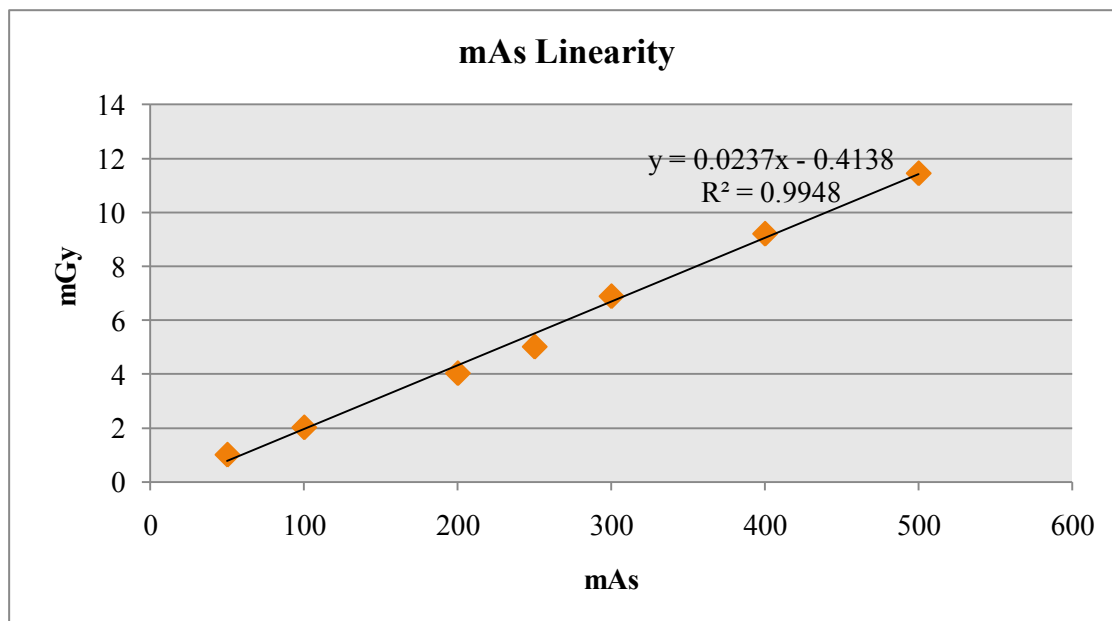


**Figure II** The relationship of mGy and mAs

**Comments:** Pass

### 9. Linearity of CT Numbers

**Method:** Set up the catphan phantom as described in beam alignment. Select the section containing the test objects of different CT numbers. Select the head technique and perform a single transverse scan. Select a region of interest (ROI) of sufficient size to cover the test objects. Place the ROI in the middle of each test object and record the mean CT number.

**Technique:** 120 kVp, 250 mA, 1 sec, 180mm SFOV, slice collimation 8 mm.

**Tolerance:** R-square between measured CT number and linear attenuation coefficient ( $\mu$ ) more than 0.9

### Results:

Material	Expected CT no. (HU)	Measured CT no. (HU)	$\mu(\text{cm}^{-1})$
Air(inferior)	-1000	-984.7	0
Air(superior)	-1000	-943.7	0
Acrylic	120	114.7	0.184
Polystyrene	-35	-41.9	0.162



LDPE	-100	-98.9	0.151
PMP	-200	-186.5	0.136
Delrin	340	309.6	0.217
Teflon	990	913.5	0.305

**Note:** Expected CT numbers are either the predicted ones or the ones obtained during the previous annual measurement.

**Comments:** Pass

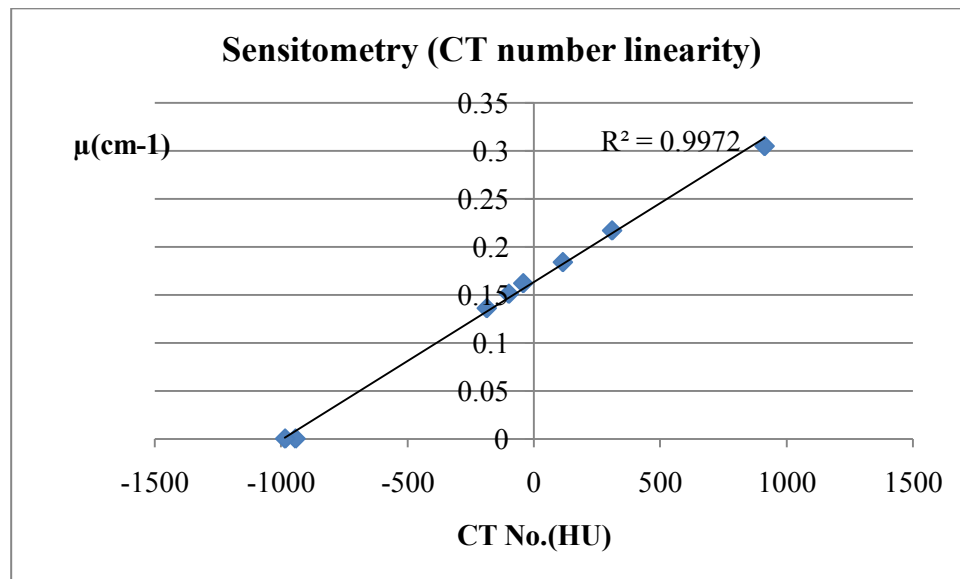


**Figure III** Linearity of CT number

## 10. Accuracy of Distance Measurement

**Purpose:** To test accuracy of Distance Measurement and for circular symmetry of the CT image

**Method:** Set up the catphan phantom as described in beam alignment. Select the section containing the test accuracy of distance measurement. Select the head technique and perform a single transverse scan. Measured object in x and y axes.

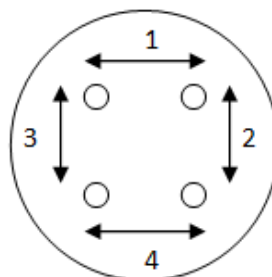


**Figure III** Accuracy

**Results:**

Position	Indicate (mm)	Measured (mm)	Different (mm)
1	50	49.9	0.1
2	50	49.9	0.1
3	50	50.3	0.3
4	50	49.9	0.1

**Comment:** Pass

**11. Image uniformity**

**Method:** Set up the catphan phantom as described in beam alignment. Select the section containing the image uniformity module. Select the head technique. Perform a single transverse scan. Measure the mean value and the corresponding standard deviations in CT numbers within a region of interest (ROI). These measurements are taken from different locations within the scan field.

**Technique:** 120 kVp, 600 mA, 1.5 sec, 200 mm FOV

**Tolerance:** 5 HU

**Results:**

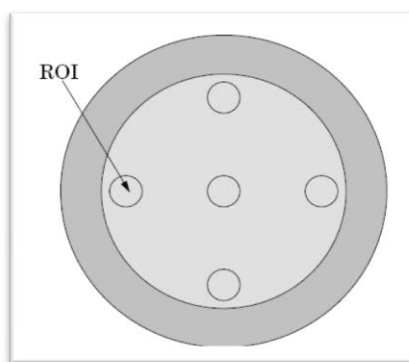


**Figure IV** Image Uniformity

Position	CT number (HU)	SD	Different (HU)
Center	2.85	3.02	0
3 o'clock	3.57	2.24	0.72
6 o'clock	2.82	2.53	0.03
9 o'clock	3.55	2.37	0.70
12 o'clock	4.30	2.35	1.45

$$*Different = |CT\ number\ center - CT\ number\ peripheral|$$

**Comment:** Pass

## 12. High Contrast Resolution

**Method:** Set up the catphan phantom as described in beam alignment. Select the section containing the high resolution test objects. Select the head technique. Perform a single transverse scan. Select the area containing the high resolution test objects and zoom as necessary. Select appropriate window and level for the best visualization of the test objects. Record the smallest test object visualized on the film.

**Technique:** 120 kVp, 600 mA, 1.5 sec, 200 mm FOV

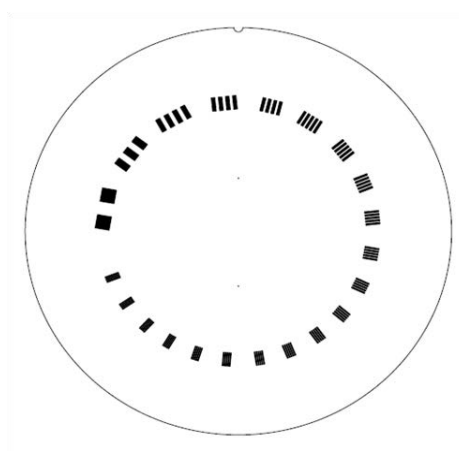


**Figure V** High contrast resolution

### Results:

Slice Thickness in mm	Resolution
8	7 lp/cm (0.071 mm)

## 13. Low Contrast Detectability

**Method:** Select the section containing the low resolution test objects in the mini phantom. Perform a single transverse scan utilizing the same technique as high resolution.

**Technique:** 120 kVp, 600 mA, 1.5 sec, 200 mm FOV, slice collimation 8 mm

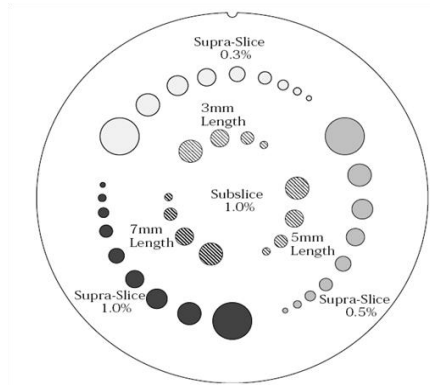


Figure VI Low contrast detectability

**Results:**

Supra-slice	Nominal target contrast levels	Hole	%Contrast
	0.30%	6	1.5
	0.50%	8	1.5
	1%	9	2
Sub-slice	Nominal target contrast levels	Hole	%Contrast
	3 mm Length	4	3
	5 mm Length	4	5
	7 mm Length	4	7

**14. Radiation Profile width**

**Purpose:** To Determine the accuracy of the slice thickness.

**Method:** Set up the catphan phantom as described in beam alignment. Select the section containing the accuracy of the slice thickness test objects. Select the head technique. Perform scan following catphan manual in each slice collimation. Calculate the real slice thickness.

**Technique:** 120 kVp, 600 mA, 1.5 sec

**Tolerance:** should be < 1mm

**Results:**

Slice Thickness(mm)	1	2	3	4	5	8
Peak	605	368	303	233	215	168
B.G.	85.99	85.89	90	85.89	89	88
Net Peak (NP.)	519.01	282.11	213	147.11	126	80
50% NP.	259.5	141.01	107	73.55	63	40
H.M. (50%NP. + B.G.)	345.49	226.9	197	159.47	152	128

<b>FWHM L1</b>	2.6	4.3	6.6	9.5	11.2	18.3
<b>FWHM L2</b>	2.6	4.7	6.6	9.0	11.7	19.2
<b>FWHM L3</b>	2.6	4.7	6.6	9.0	11.7	18.7
<b>FWHM L4</b>	2.6	4.7	7.0	9.0	11.2	18.3
<b>Average FWHM</b>	2.6	4.6	6.7	9.1	11.5	18.6
<b>SL = (Average FWHM x 0.42)</b>	1.09	1.93	2.81	3.83	4.81	7.82

---

**Comment:** Pass

**Purpose:** To Determine the maximum z-axis coverage

**Method:** Position the water phantom centered in the gantry. Use Gafchromic film inserted to the center slot of phantom. Open maximum detector array (320x0.5 mm), obtain one scan using typical head technique.

**Technique** 120 kVp, 200 mA, 1 sec

**Results:**

---

**Maximum z-axis coverage**

16 cm

**Measured FWHM**

17.3 cm

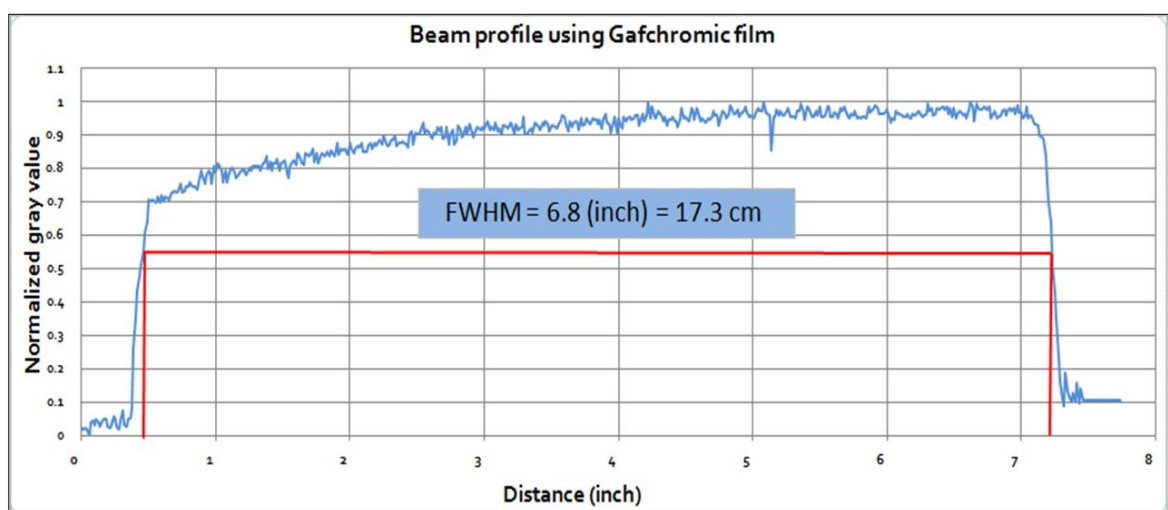


**Figure VII** Beam profile using Gafchromic film

## Appendix C: Patient information sheet

### เอกสารข้อมูลคำอธิบายสำหรับผู้ป่วยที่เข้าร่วมการวิจัย (Patient information sheet)

การวิจัยเรื่อง ปริมาณรังสีและคุณภาพของภาพในการตรวจหลอดเลือดโคโรนารี จากเครื่องคอมพิวเตอร์โทโมกราฟี ชนิด 320 หัววัด

เรียน ผู้เข้าร่วมโครงการวิจัยทุกท่าน

ท่านได้รับเชิญให้เข้าร่วมในโครงการวิจัยนี้เนื่องจากท่านเป็นผู้ป่วยที่เข้ามารับการตรวจหลอดเลือดหัวใจโคโรนารีโดยใช้เครื่องเอกซเรย์คอมพิวเตอร์ชนิด 320 หัววัดเพื่อประเมินปริมาณรังสีที่ได้รับจากการตรวจและคุณภาพของภาพเพื่อการวินิจฉัย ก่อนที่ท่านจะตัดสินใจเข้าร่วมในการศึกษาวิจัยดังกล่าว ขอให้ท่านอ่านเอกสารฉบับนี้อย่างถี่ถ้วน เพื่อให้ท่านได้ทราบถึงเหตุผลและรายละเอียดของการศึกษาวิจัยในครั้งนี้ หากท่านมีข้อสงสัยใดๆ เพิ่มเติม กรุณาซักถามจากทีมงานของแพทย์ผู้ทำวิจัย หรือแพทย์ผู้ร่วมทำวิจัยซึ่งจะเป็นผู้สามารถตอบคำถามและให้ความกระจ่างแก่ท่านได้

ท่านสามารถขอคำแนะนำในการเข้าร่วมโครงการวิจัยนี้จากครอบครัว เพื่อน หรือแพทย์ประจำตัวของท่านได้ ท่านมีเวลาอย่างเพียงพอในการตัดสินใจโดยอิสระ ถ้าท่านตัดสินใจแล้วว่า จะเข้าร่วมในโครงการวิจัยนี้ ขอให้ท่านลงนามในเอกสารแสดงความยินยอมของโครงการวิจัยนี้

ปัจจุบันการตรวจ วินิจฉัย หัวใจและหลอดเลือดหัวใจด้วยเครื่องเอกซเรย์คอมพิวเตอร์ (Coronary Computed Tomographic Angiography) มีความสำคัญอย่างยิ่ง เนื่องจากการตรวจที่ไม่ลุกล้ำเข้าไปในตัวผู้ป่วย ทำให้ลดอัตราการเสียชีวิตและทุพพลภาพได้มากกว่าการตรวจหัวใจและหลอดเลือดวิธีเดิม คือการฉีด สารทึบรังสีดูหลอดเลือดหัวใจโดยตรง (Conventional Angiography) รวมทั้งปริมาณรังสีที่ผู้ป่วยได้รับยังน้อยกว่า ด้วย จึงได้มีการพัฒนาเครื่องเอกซเรย์คอมพิวเตอร์ให้มีประสิทธิภาพมากขึ้น เพื่อให้ลดเวลาในการตรวจและเพิ่มคุณภาพของภาพทำให้การวินิจฉัยมีประสิทธิภาพมากยิ่งขึ้น เครื่องเอกซเรย์คอมพิวเตอร์เป็นการสร้างภาพตัดขวางของร่างกายโดยใช้รังสีเอ็กซ์ ซึ่งปัจจุบันได้มีการพัฒนาการของเครื่องตรวจให้สามารถตรวจได้อย่างรวดเร็วดังที่กล่าวมาแล้ว ผู้ป่วยนอนบนเตียงตรวจขณะเตียงเลื่อนเข้า-ออกผ่านเครื่อง โดยในเครื่องเอกซเรย์คอมพิวเตอร์ชนิด 320 หัววัด มีการเพิ่มจำนวนหัววัดมากถึง 320 หัววัด เวลาการหมุนของแกนทรี (gantry) 0.35 วินาที เพิ่มรายละเอียด (temporal and spatial resolution) ทำให้ภาพที่ได้มีคุณภาพดียิ่งขึ้น

การศึกษาวินิจฉัยในครั้งนี้ มีวัตถุประสงค์เพื่อศึกษาปริมาณรังสีที่ผู้ป่วยได้รับและคุณภาพของภาพจากการตรวจหลอดเลือดหัวใจโคโรนารี ในเครื่องเอกซเรย์คอมพิวเตอร์ชนิด 320 หัววัด

หลังจากท่านให้ความยินยอมที่จะเข้าร่วมในโครงการวิจัยนี้ ผู้วิจัยจะขอตรวจประเมินปริมาณรังสีและคุณภาพของภาพจากการตรวจหลอดเลือดหัวใจโคโรนารี ในเครื่องเอกซเรย์คอมพิวเตอร์ชนิด 320 หัววัด โดยการตรวจหลอดเลือดหัวใจโคโรนารี นั้นมีขั้นตอนดังนี้

- ดื่มน้ำงดอาหาร อย่างน้อย 4-6 ชั่วโมง
- รับประทานยาได้ตามปกติ ยกเว้น ผู้ป่วยเบาหวานในห้วงยามเบาหวานในวันตรวจ
- เจ้าหน้าที่ทำการซักประวัติการแพ้สารทึบรังสี แพ้อาหารทะเล แพ้ยาเป็นโรคมุมิแพ้ เป็นโรคหอบหืดรุนแรง โรคหัวใจ โรคเกี่ยวกับไต
- พยาบาลจะให้สารน้ำผ่านทางหลอดเลือดบริเวณข้อพับแขน เพื่อใช้สำหรับการฉีดสารทึบรังสี
- ในกรณีที่ผู้ป่วยมีอาการเต้นของหัวใจมากกว่า 65 ครั้งต่อนาที อาจมีความจำเป็นต้องให้ยาลดอัตราการเต้นของหัวใจ ก่อนตรวจครั้งถึงหนึ่งชั่วโมง
- ในระหว่างการตรวจ ผู้ป่วยต้องปฏิบัติตามคำแนะนำของเจ้าหน้าที่ เช่น การหายใจเข้า-ออก และการกลั้นหายใจ เพื่อให้ได้ภาพที่คมชัด

จากนั้นผู้วิจัยจะทำการบันทึกค่าปัจจัย (Parameters) ต่างๆที่เกี่ยวข้องในการตรวจเพื่อนำไปประเมินปริมาณรังสีที่ผู้ป่วยได้รับ และนำภาพที่ได้จากการตรวจให้รังสีแพทย์ประเมินคุณภาพของภาพ

#### ความรับผิดชอบของผู้ป่วยอาสาสมัครผู้เข้าร่วมในโครงการวิจัย

เพื่อให้งานวิจัยนี้ประสบความสำเร็จ ผู้ทำวิจัยใคร่ขอความความร่วมมือจากท่าน โดยจะขอให้ท่านปฏิบัติตามคำแนะนำของผู้ทำวิจัยอย่างเคร่งครัด รวมทั้งแจ้งอาการผิดปกติต่าง ๆ ที่เกิดขึ้นกับท่านระหว่างที่ท่านเข้าร่วมในโครงการวิจัยให้ผู้ทำวิจัยได้รับทราบ

#### ความเสี่ยงที่อาจได้รับ

เนื่องจากเป็นตรวจวินิจฉัยโดยใช้รังสีเอกซ์ ผู้ป่วยจึงอาจมีความเสี่ยงจากรังสีที่ได้รับและอาจมีความเสี่ยงเนื่องจากการแพ้สารทึบรังสีที่ฉีดเข้าไปในร่างกาย รวมถึงอาการข้างเคียง เช่น ร้อนไปทั่วตัว ผื่นคัน แน่นหน้าอก หายใจไม่ออก และความไม่สบายที่ยังไม่มีการรายงานด้วย ดังนั้นระหว่างที่ท่านอยู่ในโครงการวิจัยจะมีการติดตามดูแลสุขภาพของท่านอย่างใกล้ชิด กรุณาแจ้งผู้ทำวิจัยในกรณีที่พบอาการดังกล่าวข้างต้น หรืออาการอื่น ๆ ที่พบร่วมด้วย ระหว่างที่อยู่ในโครงการวิจัย ถ้ามีการเปลี่ยนแปลงเกี่ยวกับสุขภาพของท่าน ขอให้ท่านรายงานให้ผู้ทำวิจัยทราบโดยเร็ว

### ความเสี่ยงที่ได้รับจากการฉีดสารทึบรังสี

สารทึบรังสี หรือ Contrast media เป็นสารเคมีที่เมื่อฉีดเข้าไปในร่างกาย สามารถเพิ่มความแตกต่างระหว่างสีขาวและสีดำ (contrast) ในการถ่ายภาพอวัยวะภายในด้วยเอกซเรย์ หรือเอกซเรย์คอมพิวเตอร์ ภาพที่ได้จะมีความชัดเจนมากขึ้น และสามารถบอกตำแหน่งของ รอยโรค การอุดตัน หรือบวมโต รังสีที่ฉีดปกติของอวัยวะภายในได้ดีขึ้น สารทึบรังสีนี้สามารถใช้กับร่างกายหลาย ๆ ส่วนด้วยกัน เช่น สมอง หัวใจ กระดูกสันหลัง ระบบทางเดินปัสสาวะ ระบบหลอดเลือด เช่น ใช้ในการตรวจแยกภาวะหลอดเลือดสมองแตกหรืออุดตัน ตรวจหาเนื้องอกในสมอง ตรวจหาการตีตันของหลอดเลือดต่าง ๆ ดูว่าหลอดเลือดหัวใจตีตันมากน้อยเพียงใด ดูระบบทางเดินปัสสาวะเพื่อหาการอุดตัน ดูการกตบเส้นประสาทของกระดูกไขสันหลัง เป็นต้น โดยสารทึบรังสีที่ใช้ในทางการแพทย์มีอยู่ 2 ชนิด คือ ชนิดแตกตัวเป็นไอออน (ionic contrast media) และชนิดไม่แตกตัวเป็นไอออน (non-ionic contrast media) โดยในงานวิจัยครั้งนี้ท่านจะได้รับการฉีดสารทึบรังสีชนิดไม่แตกตัว ซึ่งมีผลข้างเคียงน้อยกว่าแต่อย่างไรก็ตาม จะมีแพทย์ เจ้าหน้าที่พยาบาล ดูแลอย่างใกล้ชิด เพื่อรับการ แจ้งจากท่าน โดยทันทีที่เกิดความผิดปกติ

### ความเสี่ยงที่ไม่ทราบแน่นอน

ท่านอาจเกิดอาการข้างเคียง หรือความไม่สบาย นอกเหนือจากที่ได้แสดงในเอกสารฉบับนี้ ซึ่งอาการข้างเคียงเหล่านี้เป็นอาการที่ไม่เคยพบมาก่อน เพื่อความปลอดภัยของท่าน ควรแจ้งผู้ทำวิจัยให้ทราบทันทีเมื่อเกิดความผิดปกติใดๆ เกิดขึ้น หากท่านมีข้อสงสัยใดๆ เกี่ยวกับความเสี่ยงที่อาจได้รับจากการเข้าร่วมในโครงการวิจัย ท่านสามารถสอบถามจากผู้ทำวิจัยได้ตลอดเวลา หากมีการค้นพบข้อมูลใหม่ ๆ ที่อาจมีผลต่อความปลอดภัยของท่านในระหว่างที่ท่านเข้าร่วมใน โครงการวิจัย ผู้ทำวิจัยจะแจ้งให้ท่านทราบทันที เพื่อให้ท่านตัดสินใจว่าจะอยู่ในโครงการวิจัยต่อไปหรือจะขอลอนตัวออกจากโครงการวิจัย

### การพบแพทย์นอกตารางนัดหมายในกรณีที่เกิดอาการข้างเคียง

หากมีอาการข้างเคียงใด ๆ เกิดขึ้นกับท่าน ขอให้ท่านรีบมาพบแพทย์ที่สถานพยาบาลทันที ถึงแม้ว่าจะอยู่นอกตารางการนัดหมาย เพื่อแพทย์จะได้ประเมินอาการข้างเคียงของท่าน และให้การรักษาที่เหมาะสมทันที หากอาการดังกล่าวเป็นผลจากการเข้าร่วมในโครงการวิจัย ท่านจะไม่เสียค่าใช้จ่าย

### ประโยชน์ที่อาจได้รับ

ท่านจะทราบปริมาณรังสีที่ท่านได้รับในการตรวจในครั้งนี้ และแพทย์ใช้เป็นข้อมูลประเมินผลของรังสีที่อาจเกิดขึ้นกับท่าน ภายหลังจากการเข้าตรวจวินิจฉัยหลอดเลือดหัวใจโคโรนารีด้วยเครื่องเอกซเรย์คอมพิวเตอร์ ชนิด 320 หัววัด ในครั้งนี้ได้ การเข้าร่วมในโครงการวิจัยของท่านครั้งนี้อาจจะลดความรุนแรงของการได้รับ



ปริมาณรังสีที่สูงในผู้ป่วยรายต่อไปที่มารับการตรวจ และ/หรือการตรวจในครั้งต่อไปของท่านได้ แต่ไม่ได้รับรองว่าสุขภาพของท่านจะต้องดีขึ้นหรือความรุนแรงของโรคลดลงอย่างแน่นอน

#### **ข้อปฏิบัติของท่านขณะที่ร่วมในโครงการวิจัย** ขอให้ท่านปฏิบัติตามดังนี้

- ขอให้ท่านให้ข้อมูลทางการแพทย์ของท่านทั้งในอดีต และปัจจุบัน แก่ผู้ทำวิจัยด้วยความสัตย์จริง
- ขอให้ท่านแจ้งให้ผู้ทำวิจัยทราบความผิดปกติที่เกิดขึ้นระหว่างที่ท่านร่วมในโครงการวิจัย
- ขอให้ท่านปฏิบัติตามคำแนะนำที่เจ้าหน้าที่หน่วยเอกเรย์คอมพิวเตอร์แนะนำขณะทำการตรวจ

#### **อันตรายที่อาจเกิดขึ้นจากการเข้าร่วมในโครงการวิจัยและความรับผิดชอบของผู้ทำวิจัย/ผู้สนับสนุนการวิจัย**

หากพบอันตรายที่เกิดขึ้นจากการวิจัย ท่านจะได้รับการรักษาอย่างเหมาะสมทันที หากพิสูจน์ได้ว่าท่านปฏิบัติตามคำแนะนำของทีมผู้ทำวิจัยแล้ว ผู้ทำวิจัย /ผู้สนับสนุนการวิจัยยินดีจะรับผิดชอบค่าใช้จ่ายในการรักษาพยาบาลของท่าน และการลงนามในเอกสารให้ความยินยอม ไม่ได้หมายความว่าท่านได้สละสิทธิ์ทางกฎหมายตามปกติที่ท่านพึงมี ในกรณีที่ท่านได้รับอันตรายใด ๆ หรือต้องการข้อมูลเพิ่มเติมที่เกี่ยวข้องกับโครงการวิจัย ท่านสามารถติดต่อกับผู้ทำวิจัยคือ นางสาวจุฑารัตน์ ถนอมพุดซา ได้ตลอด 24 ชั่วโมง ที่เบอร์ 085-2245432

#### **ค่าใช้จ่ายของท่านในการเข้าร่วมการวิจัย**

เสียค่าใช้จ่ายในการตรวจหารอยโรคของหลอดเลือดตามสิทธิของท่าน

#### **การเข้าร่วมและการสิ้นสุดการเข้าร่วมโครงการวิจัย**

การเข้าร่วมในโครงการวิจัยครั้งนี้เป็นไปโดยความสมัครใจ หากท่านไม่สมัครใจจะเข้าร่วมการศึกษาแล้ว ท่านสามารถถอนตัวได้ตลอดเวลา การขอลงนามออกจากโครงการวิจัยจะไม่มีผลต่อการดูแลสุขภาพโรคของท่านแต่อย่างใดผู้ทำวิจัยอาจถอนท่านออกจากโครงการวิจัย เพื่อเหตุผลด้านความปลอดภัยของท่าน หรือเมื่อผู้สนับสนุนการวิจัยยุติการดำเนินงานวิจัย หรือ ในกรณีดังต่อไปนี้

- ท่านไม่สามารถปฏิบัติตามคำแนะนำของผู้ทำวิจัย
- ท่านตั้งครรภ์ระหว่างที่เข้าร่วมโครงการวิจัย
- ท่านเกิดการข้างเคียง หรือความผิดปกติของผลทางห้องปฏิบัติการซึ่งอาจมีผลต่อการแพ้สารทึบรังสีได้ และไม่สามารถตรวจได้
- ท่านแพ้สารทึบรังสีที่ใช้ในการตรวจ
- ท่านต้องการปรับเปลี่ยนการตรวจด้วยวิธีอื่น

## การปกป้องรักษาข้อมูลความลับของผู้ป่วย

ข้อมูลนี้อาจนำไปสู่การเปิดเผยตัวท่าน จะได้รับการปกปิดและจะไม่เปิดเผยแก่สาธารณชน ในกรณีที่ผลการวิจัยได้รับการตีพิมพ์ ชื่อและที่อยู่ของท่านจะต้องได้รับการปกปิดอยู่เสมอ โดยจะใช้เฉพาะรหัสประจำโครงการวิจัยของท่าน

จากการลงนามยินยอมของท่านผู้ทำวิจัย และผู้สนับสนุนการวิจัยสามารถเข้าไปตรวจสอบบันทึกข้อมูลทางการแพทย์ของท่านได้แม้จะสิ้นสุดโครงการวิจัยแล้วก็ตาม หากท่านต้องการยกเลิกการให้สิทธิ์ดังกล่าว ท่านสามารถแจ้ง หรือเขียนบันทึกขอยกเลิกการให้คำยินยอม โดยส่งไปที่ นางสาว จุฑารัตน์ น้ ้นถนอมพุดชา 943 รพ. พญาไท 2 ถนนพหลโยธิน แขวงสามเสนใน เขตพญาไท กรุงเทพฯ 10400 และท่านสามารถติดต่อผู้วิจัยได้ 24 ชั่วโมงที่หมายเลข 085-2245432

หากท่านขอยกเลิกการให้คำยินยอมหลังจากที่ท่านได้เข้าร่วมโครงการวิจัยแล้ว ข้อมูลส่วนตัวของท่านจะไม่ถูกบันทึกเพิ่มเติม อย่างไรก็ตามข้อมูลอื่น ๆ ของท่านอาจถูกนำมาใช้เพื่อประเมินผลการวิจัย และท่านจะไม่สามารถกลับมาเข้าร่วมในโครงการนี้ได้อีก ทั้งนี้เนื่องจากข้อมูลของท่านที่จำเป็นสำหรับใช้เพื่อการวิจัยไม่ได้ถูกบันทึก จากการลงนามยินยอมของท่านแพทย์ผู้ทำวิจัยสามารถบอกรายละเอียดของงานที่เกี่ยวกับการเข้าร่วมโครงการวิจัยนี้ให้แก่แพทย์ผู้รักษาท่านได้

สิทธิของผู้เข้าร่วมในโครงการวิจัย ในฐานะที่ท่านเป็นผู้เข้าร่วมในโครงการวิจัย ท่านจะมีสิทธิ์ดังต่อไปนี้

1. ท่านจะได้รับทราบถึงลักษณะและวัตถุประสงค์ของการวิจัยในครั้งนี้
2. ท่านจะได้รับการอธิบายเกี่ยวกับระเบียบวิธีการของการวิจัยทางการแพทย์ รวมทั้งยาและอุปกรณ์ที่ใช้ในการวิจัยครั้งนี้
3. ท่านจะได้รับการอธิบายถึงความเสี่ยงและความไม่สบายที่จะได้รับจากการวิจัย
4. ท่านจะได้รับการอธิบายถึงประโยชน์ที่ท่านอาจจะได้รับจากการวิจัย
5. ท่านจะได้รับการเปิดเผยถึงทางเลือกในการรักษาด้วยวิธีอื่น ยา หรืออุปกรณ์ซึ่งมีผลดีต่อท่านรวมทั้งประโยชน์และความเสี่ยงที่ท่านอาจได้รับ
6. ท่านจะได้รับทราบแนวทางในการรักษา ในกรณีที่พบโรคแทรกซ้อนภายหลังการเข้าร่วมในโครงการวิจัย
7. ท่านจะมีโอกาสได้ซักถามเกี่ยวกับงานวิจัยหรือขั้นตอนที่เกี่ยวข้องกับงานวิจัย
8. ท่านจะได้รับทราบว่า การยินยอมเข้าร่วมในโครงการวิจัยนี้ ท่านสามารถขอลถอนตัวจากโครงการเมื่อไรก็ได้ โดยผู้เข้าร่วมในโครงการวิจัยสามารถขอลถอนตัวจากโครงการ โดยไม่ได้รับผลกระทบใด ๆ ทั้งสิ้น
9. ท่านจะได้รับสำเนาเอกสารใบยินยอมที่มีทั้งลายเซ็นและวันที่

10. ท่านจะได้โอกาสในการตัดสินใจว่าจะเข้าร่วมในโครงการวิจัยหรือไม่ก็ได้ โดยปราศจากการใช้อิทธิพล บังคับข่มขู่ หรือการหลอกลวง

หากท่านไม่ได้รับการชดเชยอันควรต่อการบาดเจ็บหรือเจ็บป่วยที่เกิดขึ้นโดยตรงจากการวิจัย หรือท่าน ไม่ได้รับการปฏิบัติตามที่ปรากฏในเอกสารข้อมูลคำอธิบายสำหรับผู้เข้าร่วมในการวิจัย ท่านสามารถร้องเรียนได้ ที่ คณะกรรมการจริยธรรมการวิจัย คณะแพทยศาสตร์ จุฬาลงกรณ์มหาวิทยาลัย ตึกอำนวยการ 3 ชั้น 3 โรงพยาบาลจุฬาลงกรณ์ ถนนพระราม 4 ปทุมวัน กรุงเทพฯ 10330 โทร 0-2256-4455 ต่อ 14, 15 ในเวลาราชการ

ขอขอบคุณในการร่วมมือของท่านมา ณ  
โอกาสนี้

Study No.....

**ใบยินยอมเข้าร่วมการวิจัย (Consent Form)**

การวิจัยเรื่อง ปริมาณรังสีและคุณภาพของภาพในการตรวจหลอดเลือดโคโรนารี จากเครื่อง คอมพิวเตอร์ โทโมกราฟฟี ชนิด 320 หัววัด

วันที่ให้คำยินยอม วันที่.....เดือน.....พ.ศ. ....

ข้าพเจ้า นาย/นาง/นางสาว.....ที่อยู่.....

ได้อ่านรายละเอียดจากเอกสารข้อมูลสำหรับผู้เข้าร่วมโครงการวิจัยวิจัยที่แนบมาฉบับวันที่.....  
และข้าพเจ้ายินยอมเข้าร่วมโครงการวิจัยโดยสมัครใจ

ข้าพเจ้าได้รับสำเนาเอกสารแสดงความยินยอมเข้าร่วมในโครงการวิจัยที่ข้าพเจ้าได้ลงนาม และ วันที่ พร้อมด้วยเอกสารข้อมูลสำหรับผู้เข้าร่วมโครงการวิจัย ทั้งนี้ก่อนที่จะลงนามในใบยินยอมให้ทำการวิจัยนี้ ข้าพเจ้าได้รับการอธิบายจากผู้วิจัยถึงวัตถุประสงค์ของการวิจัย ระยะเวลาของการทำวิจัย วิธีการวิจัย อันตราย หรืออาการที่อาจเกิดขึ้นจากการวิจัย หรือจากยาที่ใช้ รวมทั้งประโยชน์ที่จะเกิดขึ้นจากการวิจัย และแนวทางรักษาโดยวิธีอื่นอย่างละเอียด ข้าพเจ้ามีเวลาและโอกาสเพียงพอในการซักถามข้อสงสัยจนมีความเข้าใจอย่างดีแล้ว โดยผู้วิจัยได้ตอบคำถามต่าง ๆ ด้วยความเต็มใจไม่ปิดบังซ่อนเร้นจนข้าพเจ้าพอใจ ข้าพเจ้ามีสิทธิ ที่จะบอกเลิกเข้าร่วมในโครงการวิจัยเมื่อใดก็ได้ โดยไม่จำเป็นต้องแจ้งเหตุผล และการบอกเลิกการเข้าร่วมการวิจัยนี้ จะไม่มีผลต่อการรักษาโรคหรือสิทธิอื่น ๆ ที่ข้าพเจ้าจะพึงได้รับต่อไป ผู้วิจัยรับรองว่าจะเก็บข้อมูลส่วนตัวของข้าพเจ้าเป็นความลับ และจะเปิดเผยได้เฉพาะเมื่อได้รับการยินยอมจากข้าพเจ้าเท่านั้น บุคคลอื่นในนามของบริษัทผู้สนับสนุนการวิจัย คณะกรรมการพิจารณาจริยธรรมการวิจัยในคน สำนักงานคณะกรรมการอาหารและยาอาจได้รับอนุญาตให้เข้ามาตรวจและประมวลข้อมูลของผู้เข้าร่วมวิจัย ทั้งนี้จะต้องกระทำไปเพื่อวัตถุประสงค์เพื่อตรวจสอบความถูกต้องของข้อมูลเท่านั้น โดยการตกลงที่จะเข้าร่วมการศึกษานี้ข้าพเจ้าได้ให้คำยินยอมที่จะให้มีการตรวจสอบข้อมูลประวัติทางการแพทย์ของผู้เข้าร่วมวิจัยได้

ผู้วิจัยรับรองว่าจะไม่มีการเก็บข้อมูลใด ๆ ของผู้เข้าร่วมวิจัย เพิ่มเติม หลังจากที่ข้าพเจ้าขอยกเลิก การเข้าร่วมโครงการวิจัยและต้องการให้ทำลายเอกสารและ/หรือ ตัวอย่างที่ใช้ตรวจสอบทั้งหมดที่สามารถสืบค้นถึงตัวข้าพเจ้าได้ข้าพเจ้าเข้าใจว่า ข้าพเจ้ามีสิทธิที่จะตรวจสอบหรือแก้ไขข้อมูลส่วนตัวของข้าพเจ้าและสามารถยกเลิกการให้สิทธิในการใช้ข้อมูลส่วนตัวของข้าพเจ้าได้ โดยต้องแจ้งให้ผู้วิจัยรับทราบ ข้าพเจ้าได้ตระหนักว่าข้อมูลในการวิจัยรวมถึงข้อมูลทางการแพทย์ของข้าพเจ้าที่ไม่มีการเปิดเผยชื่อ จะผ่านกระบวนการต่าง ๆ เช่น การเก็บข้อมูล การบันทึกข้อมูลในแบบบันทึกและในคอมพิวเตอร์ การตรวจสอบ การวิเคราะห์ และการรายงานข้อมูลเพื่อวัตถุประสงค์ทางวิชาการ รวมทั้งการใช้ข้อมูลทางการแพทย์ในอนาคตหรือการวิจัยทางด้านเภสัชภัณฑ์ เท่านั้น

ข้าพเจ้าได้อ่านข้อความข้างต้นและมีความเข้าใจดีทุกประการแล้ว ยินดีเข้าร่วมในการวิจัยด้วยความเต็มใจ จึงได้ลงนามในเอกสารแสดงความยินยอมนี้

ลงนาม.....ผู้ให้ความยินยอม

(.....)

วันที่ .....เดือน.....พ.ศ. ....

ข้าพเจ้ารังสีแพทย์ผู้วินิจฉัยโรคหลอดเลือดโคโรนารี ด้วยเครื่องเอกซเรย์คอมพิวเตอร์ชนิด 320 หัววัด  
ได้รับทราบจากผู้ทำวิจัยถึงวัตถุประสงค์ของการวิจัย วิธีการวิจัย และอุปกรณ์ที่ใช้ รวมทั้งประโยชน์ที่จะเกิดขึ้น  
จากการวิจัยอย่างละเอียด ซึ่งอุปกรณ์ชนิดนี้จะไม่รบกวนหรือเป็นอุปสรรค ในขณะที่ทำการตรวจแต่อย่าง  
ใด

ลงนาม .....รังสีแพทย์

(.....)

วันที่ .....เดือน.....พ.ศ. ....

ลงนาม.....ผู้ทำวิจัย

ลงนาม.....พยาน

(.....)

(.....)

วันที่ .....เดือน.....พ.ศ. ....

วันที่ .....เดือน.....พ.ศ. ....

**VITAE**

<b>NAME</b>	Miss Jutharat Thanomphudsa
<b>SEX</b>	Female
<b>NATIONALITY</b>	Thai
<b>DATE OF BIRTH</b>	20 February 1984
<b>PLACE OF BIRTH</b>	Nakhonratchasima
<b>INSTITUTIONS ATTENDED</b>	Mahidol University, 2005: Bachelor of Science (Radiological Technology) Phyathai Hospital, 2006: Certificate of sonography
<b>HOME ADDRESS</b>	943 Phyathai2 Hospital Phaholyothin Rd. Samsennai Phyathai Bangkok, Thailand 10400 Tel. 085-2245432